

# Planning of integrated mobility-on-demand and urban transit networks

Pramesh Kumar<sup>\*a</sup>, Alireza Khani<sup>a</sup>

<sup>a</sup>*Department of Civil, Environmental and Geo-Engineering, University of Minnesota, Twin Cities, MN*

---

## Abstract

We envision a multimodal transportation system where Mobility-on-Demand (MoD) service is used to serve the first mile and last mile of transit trips. For this purpose, the current research formulates an optimization model for designing an integrated MoD and urban transit system. The proposed model is a mixed-integer non-linear programming model that captures the strategic behavior of passengers in a multimodal network through a passenger assignment model. It determines which transit routes to operate, the frequency of the operating routes, the fleet size of vehicles required in each transportation analysis zone to serve the demand, and the passenger flow on both road and transit networks. A Benders decomposition approach with several enhancements is proposed to solve the given optimization program. Computational experiments are presented for the Sioux Falls multimodal network. The results show a significant improvement in the congestion in the city center with the introduction and optimization of the integrated transportation system. It improves the total number of served passengers and their level of service in comparison to the base optimized transit system. Finally, managerial insights for deploying such multimodal service are provided.

*Keywords:* Transit network design problem (TNDP), mobility-on-demand (MoD), first mile last mile (FMLM), multimodal passenger assignment, Benders decomposition

---

---

\*Corresponding author

<sup>1</sup>Email: kumar372@umn.edu

<sup>2</sup>Tel: (716) 903-2366

<sup>3</sup>Web: <http://umntransit.weebly.com/>

# 1. Introduction

The introduction of Mobility-on-Demand (MoD) services such as Uber, Lyft, and others as transportation alternatives has created many opportunities as well as challenges. On one hand, they provide a seamless mobility service with just a few taps on a cellphone application. On the other hand, it has increased congestion in densely populated areas due to an increase in the relocation and pickup trips made by the participating drivers in the network (Laris 2019). Furthermore, the transportation agencies envision the introduction of Autonomous Vehicles as a shared mobility service in the near future (Motavalli 2020), which would lead to severe congestion in densely populated areas as predicted by various simulation studies (Levin and Boyles 2015, Fagnant et al. 2016, Levin et al. 2017).

Public transportation, which can carry multiple passengers, is widely considered as a practical solution to the congestion problem by reducing vehicle-miles traveled (VMT) on roads (Aftabuzaman et al. 2015). However, due to its fixed routes and schedules, limited network coverage, and waiting time, sometimes, it is less attractive to travelers in comparison to the auto mode. The limited network coverage makes it difficult or sometimes impossible to access transit service in some areas. This inaccessibility problem is also known as the *first mile/last mile (FMLM) problem for transit*. The problem is commonly faced by travelers commuting from low-density areas where transit service is not available or less frequent because of the economic in-viability of providing such service.

A few studies have argued that the Mobility-on-demand service provided using autonomous vehicles would become a competitor of public transit mode (Chen and Kockelman 2016, Levin and Boyles 2015, Mo et al. 2020), reducing its ridership, and other studies have even raised the question of whether urban mobility is possible without the classical public transit service (OECD 2015, Mendes et al. 2017). However, Salazar et al. 2018 showed that the integration of the MoD system with transit could help in achieving better results, such as a significant reduction in travel time, emissions, and costs as compared to the standalone MoD system. Through the current research, we also envisage an integrated MoD and transit system that aims to achieve the following potential benefits:

1. Providing fast and reliable mobility in low-density areas (i.e., by providing a first mile/last mile service) by means of characteristics of MoD service such as demand responsiveness, fleet repositioning, and reachability.
2. Allocation of resources from less congested areas to providing high-frequency transit service in congested areas through such integration.
3. Using existing transit infrastructure to reduce the number of vehicles needed for serving trips.

37 4. Reducing congestion and carbon emissions in the network, improving the mobility of travelers,  
38 and reducing the overall cost of providing transit service.

39 To achieve the above-mentioned benefits, we focus on the strategic planning of the transporta-  
40 tion network that allows for intermodal trips with the first or last leg of the trips being served by  
41 the MoD service. To be specific, we try to answer questions such as which transit routes to operate  
42 when MoD vehicles are deployed to serve the FMLM connection, what should be the size of the  
43 vehicle fleet to be deployed, and what should be the frequency of operating transit routes. We  
44 attempt to answer these questions and make the following contributions through this article:

- 45 1. Propose a passenger assignment model that predicts the travel behavior of passengers in a  
46 multimodal network. This step extends the idea of a hyperpath transit assignment model  
47 proposed by Spiess and Florian 1989 to a multimodal transportation system with on-demand  
48 services.
- 49 2. Develop an optimization model to decide which transit routes to operate, frequency of oper-  
50 ating transit routes, and MoD fleet size required to serve the FMLM of trips.
- 51 3. Develop a fast Benders decomposition implementation that uses efficient cutting planes to  
52 solve the large instances of the current problem.
- 53 4. Conduct numerical experiments to show the efficacy of the proposed model and solution  
54 methods and discuss the steps to implement such service in practice.

## 55 2. Related work

56 The passenger journeys that consist of auto, as well as transit mode, create a new mode of  
57 transportation known as *intermodal* or *multimodal* transportation. The research on modeling mul-  
58 timodal transportation has been an active area of research for several decades (Wilson 1972). Many  
59 of these studies are focused on solving the transit FMLM problem by designing a multimodal trans-  
60 portation system. This includes designing a demand responsive transit feeder service (Wang 2017,  
61 Maheo et al. 2017, Cayford and Yim 2004, Koffman 2004, Lee and Savelsbergh 2017, Quadrifoglio  
62 et al. 2008, Shen and Quadrifoglio 2012, Li and Quadrifoglio 2009), using park-and-ride facilities  
63 (Nassir et al. 2012, Khani et al. 2012, Webb and Khani 2020), and integrating ridesharing and  
64 transit (Masoud et al. 2017, Stiglic et al. 2018, Bian and Liu 2019, Ma et al. 2019, Chen et al. 2020,  
65 Kumar and Khani 2021).

66  
67 Recently, the studies are being focused on modeling the integration of MoD and transit service  
68 for future mobility. They can be divided into two categories: simulation-based and optimization-  
69 based approaches. Under a set of assumptions on vehicle operations operations and dispatching  
70 strategies, the simulation-based studies simulate the passenger flow to assess the service quality  
71 of providing such mobility service (Gurumurthy et al. 2020). By using a four-step travel demand

72 simulation model, Levin and Boyles 2015 predicted that the transit ridership will decrease and the  
73 number of personal vehicles will sharply increase as a result of the repositioning of vehicles resulting  
74 in congestion on the network. Vakayil et al. 2017 developed a simulation model that accounts for  
75 transit frequency, transfer costs, and MoD fleet re-balancing to use MoD as the FMLM solution  
76 to the transit mode. Their results show that such an integrated system can reduce VMT in the  
77 network by up to 50%. Mendes et al. 2017 developed an event-based simulation model to compare  
78 the performance of the MoD system with the light rail system under the same demand patterns,  
79 alignment, and operating speed. They found that 150 vehicles with 12 passenger capacity would be  
80 needed to match the 39-vehicle light rail system if operated as a demand responsive system. Similar  
81 findings were also shown by the simulation model developed by Basu et al. 2018. They showed that  
82 the introduction of MoD will act as the competitor of mass transit, however, to reduce congestion  
83 and maintain a sustainable urban transportation system, it cannot replace mass transit. Shen  
84 et al. 2018 also proposes and simulates an integrated autonomous vehicle and public transporta-  
85 tion system based on the fixed modal split assumption. Using Singapore’s organizational structure  
86 and demand characteristics, they propose to preserve high-demand bus routes while re-purposing  
87 low-demand bus routes and using shared MoD as an alternative. They found that the integrated  
88 system has the potential of serving the trips with less congestion, less passenger discomfort, and  
89 economically viable service. Wen et al. 2018 included mode choice and various vehicle capacities  
90 and hailing strategies in an agent-based model to provide insights into fleet sizing and frequency of  
91 transit routes for the integrated system. A few studies have used an optimization-based approach to  
92 developing an integrated passenger flow model. Salazar et al. 2018 developed a network flow model  
93 for intermodal service that couples the interaction between MoD and transit by maximizing social  
94 welfare. Using this model, they proposed a tolling scheme for this intermodal system that helps in  
95 reducing the travel time, costs, and emissions as compared to standalone vehicle mode. Liu et al.  
96 2019 used Bayesian optimization to predict the mode choice of passengers in such a multimodal  
97 transportation system.

98

99 The above-cited studies show that an integrated MoD and transit system can provide an effi-  
100 cient mode of transportation that is sustainable, fast, eco-friendly, and economically viable. The  
101 design of such a system requires solving a *multimodal transportation network design problem* that  
102 can decide various aspects of MoD and transit modes. The problem of designing transit routes  
103 and their corresponding frequencies, which is commonly referred to as the Transit Network Design  
104 Problem (TNDP) or Line Planning Problem (LPP) in the literature, is itself a complex problem  
105 (Ceder and Wilson 1986, Baaj and Mahmassani 1991). There has been a significant amount of  
106 research in modeling TNDP and developing solution algorithms for it. For a review on transit  
107 network design literature, we refer the interested reader to Guihaire and Hao 2008. Some aspects  
108 of the multimodal network design problem have been explored in a related research problem known  
109 as *hub and arc location problem* (Mahéo et al. 2019, Campbell et al. 2005*a,b*). For example, Mahéo  
110 et al. 2019 proposed the design of a hub and shuttle public transit system in Canberra. They

111 formulated a mixed-integer program to design high-frequency bus routes between key-hubs, where  
112 the first mile or last mile of trips is covered by the shuttles. However, the hub and arc location  
113 problem have a major limitation of not able to capture passenger behavior in the transit network.  
114 Recently, a couple of studies have proposed models for the transit network design in the context  
115 of integrated MoD and transit system (Manser 2017, Pinto et al. 2020, Steiner and Irnich 2020).  
116 Pinto et al. 2020 develops a bi-level optimization model to design a transit network integrated with  
117 MoD service. The upper-level optimization problem modifies the frequency of the transit routes  
118 and determines the fleet size of MoD service and the lower-level model simulates the passenger  
119 trajectories based on a simulation-based traveler assignment model. Due to the complexity of the  
120 model, they presented a heuristic approach to solving the current problem. Steiner and Irnich 2020  
121 presents various aspects of this problem and develops a path-based mixed-integer programming  
122 model to decide which sections of the transit routes to operate and locate the transfer stops to  
123 allow for intermodal trips in the network. Due to an enormous number of possible paths in the  
124 network, they solve the current model using a branch-and-price approach.

125

126 The design of an integrated MoD and transit system is an important problem that can influence  
127 the future mobility of travelers. Recent studies have made important contributions to this complex  
128 problem but have several limitations, which we attempt to address in the current study. The  
129 motivation of the current research is outlined in the following points:

- 130 1. Before designing the integrated system, we should understand how passengers would behave  
131 in an integrated system. It is common for studies to use the classic multi-commodity flow  
132 model to predict the behavior of travelers in the network design. This may be true if passenger  
133 trajectories are completely influenced by the mobility provider. However, this is certainly not  
134 applicable in the case of transit systems when passengers try to reduce the expected travel  
135 time based on waiting time, travel time, and fare. Through this study, we extend the idea of  
136 hyperpath passenger assignment for a multimodal transportation system.
- 137 2. We develop a mixed-integer optimization model that incorporates the multimodal passenger  
138 assignment and evaluates various aspects of an integrated system. The optimization program  
139 is difficult to solve, and we need efficient techniques to solve this problem. For this purpose,  
140 an exact method based on the Benders Decomposition is proposed to solve the large-scale  
141 instances of the problem. The method improves the classic Benders decomposition strategy by  
142 precluding the infeasibility cuts and including new cuts, such as disaggregated cuts, multiple  
143 cuts, and clique/cover cuts.

144 The rest of the article is structured as follows. §3 discusses the notations and definitions used in  
145 this article. Then, we present the multimodal passenger assignment model, which is incorporated  
146 in the design model of the integrated MoD and transit system in §4. The solution algorithm to  
147 solve the design model is discussed in §5, which is followed by the results of numerical experiments

148 conducted on Sioux Falls network. Finally, conclusions and recommendations for future research  
 149 are presented in §7.

### 150 3. Preliminaries and Background

151 In this section, we get familiarize ourselves with the notations and concepts to be used in  
 152 this article. Let us begin by considering a multimodal transportation network characterized by a  
 153 digraph  $G(N, A)$ , where  $N$  denotes the set of nodes that includes road intersections  $N_R$ , transit  
 154 stops/stations  $N_T$ , and centroids of traffic analysis zones  $Z^4$  and  $A$  denotes the set of links. We  
 155 associate every node  $i \in N$  in the network with exactly one zone  $Z(i)$ . The set of links coming out  
 156 and going into a node  $i \in N$  are denote by  $FS(i) = \{(i, j) : (i, j) \in A\}$  and  $BS(i) = \{(j, i) : (j, i) \in$   
 157  $A\}$  respectively. Let  $\mathfrak{d} : N \times N \mapsto \mathfrak{R}_+$  be the distance function between two nodes in the network.  
 158 Depending on the mode, the links are also divided into three categories, namely transit, road, and  
 159 walking links represented by  $A_T, A_R$ , and  $A_W$  respectively. Let  $O \subset Z$  and  $D \subset Z$  be the subsets  
 160 of centroids representing the origins and destinations respectively. The demand between various  
 161 origin-destination pairs is represented by  $\{d_{od}\}_{(o,d) \in O \times D}$ . The overall network can be divided into  
 162 three sub-networks which are described below:

- 163 1. *Transit network*: The transit network is characterized by the subgraph  $G_T(N_T, A_T)$  which  
 164 consists of a set of candidate transit lines/routes denoted by the set  $L$ . The terms "route"  
 165 and "line" are used interchangeably throughout this article. Each line  $l \in L$  is composed of  
 166 a set of stops  $N_T^l \subset N_T$  which are connected by edges  $A_T^l \subset A_T$ . The network also consists  
 167 of transfer links  $A_T^{tr}$  between two nodes if the walking distance between those is less than the  
 168 acceptable walking distance  $\zeta$  (say 0.75mi), i.e.,  $A_T^{tr} = \{(n_1, n_2) \in N \times N : n_1 \in N_T^{l_1}, n_2 \in$   
 169  $N_T^{l_2}$  for some  $l_1, l_2 \in L$  s.t.  $l_1 \neq l_2$  and  $\mathfrak{d}(n_1, n_2) \leq \zeta\}$ .
- 170 2. *Road network*: The road network is characterized by the subgraph  $G_R(N_R, A_R)$ , where  $N_R$   
 171 denotes the set of nodes and  $A_R$  denotes the set of links in the road network.
- 172 3. *Walking links*: The walking links consists of access, egress, and mode transfer links. The  
 173 *access* and *egress links* are defined as  $A^a = \{(n_1, n_2) \in Z \times (N_T \cup N_R) : \mathfrak{d}(n_1, n_2) \leq \zeta\}$  and  
 174  $A^e = \{(n_1, n_2) \in (N_T \cup N_R) \times Z : \mathfrak{d}(n_1, n_2) \leq \zeta\}$  respectively. Similarly, the *mode transfer*  
 175 *links* are defined as  $A^m = \{(n_1, n_2) \in N_R \times N_T : \mathfrak{d}(n_1, n_2) \leq \zeta\} \cup \{(n_1, n_2) \in N_T \times N_R :$   
 176  $\mathfrak{d}(n_1, n_2) \leq \zeta\}$ . The access and egress walking links connect the centroids of various zones  
 177 with the road/transit nodes and vice-versa, whereas mode transfer links are used to transfer  
 178 between nodes of various modes.

---

<sup>4</sup>A *traffic analysis zone* (TAZ) or simply a zone is a geographical area where the demand is assumed to be concentrated on its centroid.

179 *3.1. Costs*

180 There is a subset of nodes in the network where passengers have to wait for the service. The  
 181 collection of head nodes of links in the sets  $A^a$ ,  $A_T^{tr}$ , and  $A^m$  constitutes the *waiting nodes*  $N^w$ .  
 182 Let us assume that  $c : A \mapsto \mathfrak{R}_+$  and  $w : N^w \mapsto \mathfrak{R}_+$  denote the cost (e.g., walking time, in-vehicle  
 183 time, and fare) associated with the links in  $A$  and waiting time associated with the nodes in  $N^w$   
 184 respectively. The cost of links is known beforehand (and is computed by adding the travel time  
 185 and possible fare multiplied by the value of time). On the other hand, the wait time depends on  
 186 the availability of MoD or transit service.

187 *3.2. Waiting time computation*

188 Unlike a personal vehicle, the MoD or transit service is not readily available, and passengers  
 189 have to wait to access these services. So, it is important to quantify the expected wait time of these  
 190 services, the computation of which is discussed below:

191 *3.2.1. MoD service*

192 We assume MoD operations in a network as a queuing system to compute the average waiting  
 193 time experienced by the passengers to access such service. The average wait time may not be  
 194 justified for the planning of day-to-days operations but can be used to approximate the actual wait  
 195 time experienced by the passengers for long-term strategic planning of the network, which is the  
 196 focus of the current study. Therefore, we consider a stationary state of an MoD system, where the  
 197 number of waiting customers  $\mathcal{C}$  and vacant vehicles  $\mathcal{V}$  are time-invariant. Using the Cobb-Douglas  
 198 production function, the matching time between the customers and the vacant vehicles can be  
 199 expressed as a function of  $\mathcal{C}$  and  $\mathcal{V}$ .

$$m^{c-v} = \mathcal{A}(\mathcal{V})^{\alpha_1} (\mathcal{C})^{\alpha_2} \quad (1)$$

200 where,  $\alpha_1$  and  $\alpha_2$  are defined as the elasticities of the matching function and  $\mathcal{A}$  is a parameter  
 201 specific to a zone, which is a function of the market area divided by the running speed in that zone  
 202 (Zha et al. 2016). According to Little's law, the long-term average number of customers/drivers in  
 203 a stationary system is equal to the long-term average arrival rate  $Q$  multiplied by the average wait  
 204 time ( $w^c/w^t$ ) that a customer/driver spends in the system before being matched (Zha et al. 2016).

$$\mathcal{V} = Qw^t \quad (2)$$

$$\mathcal{C} = Qw^c \quad (3)$$

205 Using (3) and assuming  $\alpha_1 = \alpha_2 \approx 1$  (Douglas 1972), we can represent the stationary state  
 206 ( $m^{c-v} = Q$ ) as below:

$$Q = \mathcal{A}\mathcal{V}(Qw^c) \quad (4)$$

$$\implies w^c = \frac{1}{\mathcal{A}\mathcal{V}} \quad (5)$$

207 Equation (5) shows that the average waiting time of customers waiting in a zone to access the MoD  
 208 service is a function of the vacant number of vehicles. To achieve the desired level of service (i.e.,  
 209 average waiting time), a transportation agency needs to provide  $\mathcal{V}$  vehicles at any point in time.

### 210 3.2.2. Transit service

211 Let us now discuss the wait time computation to access transit service at the head node of an  
 212 access or transfer link in the transit network. Let  $f : A_T \mapsto \mathfrak{R}$  be the frequency of the transit  
 213 line associated with various links of the transit network. Let  $\mathfrak{g}_i(w)$  be the probability distribution  
 214 function of the waiting time for line  $i$ . According to Larson and Odoni 1981, for the passengers  
 215 arriving randomly at a node, the probability density function of the waiting time of line  $i$  is related  
 216 to the headway or bus inter-arrival time distribution  $\mathfrak{h}_i(h)$  as:

$$\mathfrak{g}_i(w) = \frac{\int_w^\infty \mathfrak{h}_i(h) dh}{\mathbb{E}[\mathfrak{h}_i]} \quad (6)$$

217 To evaluate the waiting time distribution, we make the following assumptions:

218 **Assumption 1.** *The inter-arrival time of a transit line  $i \in L$  follows an exponential distribution*  
 219 *with rate  $f_i$ .*

220 **Assumption 2.** *Passengers want to minimize the expected wait time to get to their destination.*  
 221 *Therefore, at any node, passengers waiting to be served by the transit service have selected a list of*  
 222 *attractive transit lines that can help them to get to their destination.*

223 Both assumption 1 and 2 are common in the transit assignment literature (e.g., see Desautniers  
 224 and Hickman 2007). By using the assumption 1 and equation (6), one can evaluate the distribution  
 225 function of the wait time  $\mathfrak{g}_i(w)$  as:

$$\mathfrak{g}_i(w) = f_i e^{-f_i w}, w \geq 0 \quad (7)$$

226 **Proposition 1.** *(Spiess and Florian 1989, Gentile et al. 2005) Assuming that a passenger waiting*  
 227 *at node  $n \in N^w$  is served by the set of attractive transit lines  $FS^*(n)$  and let  $\mathfrak{F} = \sum_{j \in FS^*(n)} f_j$ .*  
 228 *With assumptions 1 and 2, the following holds:*

229 1. *The probability that a passenger would choose transit line  $i \in FS^*(n)$  is given by*

$$P_i = \frac{f_i}{\mathfrak{F}} \quad (8)$$

230 2. *The expected wait time conditional to boarding line  $i \in FS^*(n)$  is given by*

$$EW_i = \frac{f_i}{\mathfrak{F}^2} \quad (9)$$

231 3. *The probability of wait time at node  $n$  follows an exponential distribution with rate  $\mathfrak{F}$ . There-*  
 232 *fore, the expected wait time at stop  $n$  is given by  $EW_n = \frac{1}{\mathfrak{F}}$ .*



233 *Proof.* See Appendix A. □

### 234 3.2.3. Combined MoD and transit service wait time

235 Before discussing the computation of the expected wait time involving both modes, we need to  
 236 make an assumption about the wait time distribution of MoD service by utilizing the value of the  
 237 average wait time of MoD service calculated in equation (5).

238 **Assumption 3.** *The wait time distribution of MoD service for passengers waiting at node  $n$  follows*  
 239 *an exponential distribution with rate  $f_{MoD} = \mathcal{A}_{Z(n)}\mathcal{V}_{Z(n)}$ , where  $Z(n)$  is the zone associated to node*  
 240  *$n$  and  $\mathcal{V}_{Z(n)}$  is the number of vehicles deployed in zone  $Z(n)$ .*

241 A passenger waiting at the head node of an access link faces the choice between MoD or transit  
 242 mode. This is because the wait time of both services can vary based on the frequency provided,  
 243 and a passenger will include one or both modes in their strategy to reduce the overall expected  
 244 cost. This assumption simplifies the operation of MoD service as a transit service available at any  
 245 stop of the network. The following proposition evaluates the expected wait time of that passenger.

246 **Proposition 2.** *Given that the waiting time for transit and MoD mode follow an exponential*  
 247 *distribution with rate  $\mathfrak{F}$  and  $f_{MoD}$  respectively and  $\mathbb{F} = \mathfrak{F} + f_{MoD}$ , the following holds:*

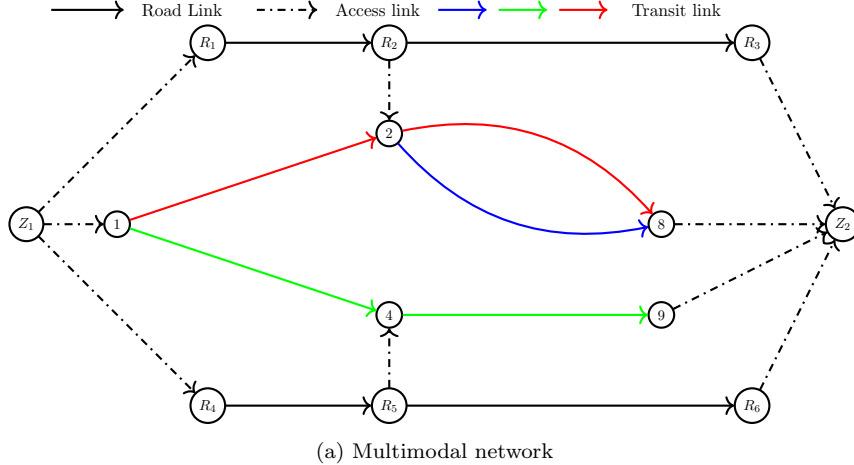
- 248 1. *The probabilities of taking transit and MoD are given by  $P_{MoD} = \frac{f_{MoD}}{\mathbb{F}}$  and  $P_{transit} = \frac{\mathfrak{F}}{\mathbb{F}}$*   
 249 *respectively.*
- 250 2. *The expected wait time of the passenger departing from an access node  $n$  served by both MoD*  
 251 *and transit service is given by  $EW_n = \frac{1}{\mathbb{F}}$*

252 *Proof.* See Appendix A. □

253 To get more insights into the wait time computation, let us consider an example. Figure 1(a)  
 254 shows an illustration of a multimodal transportation network. It consists of 2 zones, 6 nodes and  
 255 8 links as part of the road network, and 5 nodes and 10 links as part of the transit network. The  
 256 transit network has 3 transit lines (color-coded) whose frequencies are shown in Figure 1(b). There  
 257 are 100 and 50 vehicles deployed in zone 1 and 2 respectively. By using Prop 1, we can evaluate the  
 258 probability of passengers taking various transit lines in the network. For example, the probabilities  
 259 of choosing red line and green line at stop 1 are  $\frac{1/6}{1/6+1/2} = 0.25$  and  $\frac{1/2}{1/6+1/2} = 0.75$  respectively.  
 260 The expected wait time at stop 1 is equal to  $12/8 = 1.5$  minutes. Similarly, using Proposition 2,  
 261 the probabilities of choosing MoD and transit at  $Z_1$  are  $\frac{0.0017*100}{0.0017*100+8/12} = 0.2$  and 0.8 respectively  
 262 (assuming  $\mathcal{A}_1 = 0.0017$ ). The overall expected wait time at node  $Z_1$  is 1.19 minutes which is less  
 263 than 1.5 minutes by only considering transit service as part of the strategy.

264

265 We further use Proposition 1 and 2 to formulate the multimodal passenger assignment model.  
 266 For this purpose, we extend the frequency-based transit assignment model proposed by Spiess and  
 267 Florian 1989 to a multimodal transportation system. Before moving forward, we must make the  
 268 following assumptions:



(a) Multimodal network

Line	Frequency	Zone	Vehicles
Red	1/6	$Z_1$	100
Green	1/2	$Z_2$	50
Blue	1/3		

(b) Frequency and number of vehicles

Figure 1: An illustrative example of a multimodal network

269 **Assumption 4.** (a) *Ridepooling is not allowed, i.e., the MoD service serves one passenger at a*  
 270 *time.*

271 (b) *The transit lines are assumed to have unlimited capacity.*

272 (c) *Passengers want to reduce their expected generalized travel cost consisting of travel time, wait*  
 273 *time, and fare to get to their destination.*

274 The ridepooling problem requires matching of customers using a specific algorithm. This is an  
 275 important aspect to accurately estimate the cost of day-to-day operations. Nevertheless, ignoring  
 276 ridepooling will give us an upper bound on the number of vehicles required to serve various zones.  
 277 The modeling of passenger behavior while incorporating the capacity constraints (congestion) is  
 278 a difficult problem. The congestion is important to consider since it causes denied boarding,  
 279 which leads to increased waiting time, travel time, and discomfort. Several authors have tried  
 280 to include congestion into frequency-based transit assignment models through various approaches,  
 281 namely, discomfort function (Spiess and Florian 1989), effective frequency (De Cea and Fernández  
 282 1993, Cominetti and Correa 2001, Cepeda et al. 2006, Leurent et al. 2014), and failure-to-board  
 283 probabilities (Kurauchi et al. 2003). Despite the effort, there is no tractable closed-form of congested  
 284 frequency-based transit assignment model. On the other hand, it would not be ideal to include  
 285 transit vehicle capacity constraints into the assignment program (e.g., in Szeto and Jiang 2014)  
 286 because doing so may lead to unrealistic passenger behavior, which previous studies on congested  
 287 frequency-based transit assignments were trying to avoid. Therefore, we use an uncapacitated  
 288 assignment for the design problem. Assumption 4(c) is a common in the assignment literature.  
 289 The relaxation of above assumptions are research topics in their own right, therefore, a discussion

290 on possible ways to relax them is provided in §7. To proceed further, let us define a variable  
 291  $\{g_{ik}\}_{i \in N, k \in D}$  as below:

$$g_{ik} = \begin{cases} d_{ik}, & \text{if } i \neq k, (i, k) \in O \times D \\ -\sum_{o \in O} d_{ok}, & \text{if } i = k \\ 0, & \text{otherwise} \end{cases}$$

Furthermore, let us denote  $v_{ak}$  and  $W_{ik}$  as the flow of passengers on link  $a \in A$  and waiting at node  $i \in N^w$  resp. destined to  $k \in D$ . The assignment optimization program is presented below:

$$\underset{v, W}{\text{minimize}} \quad \sum_{k \in D} \left( \sum_{a \in A} c_a v_{ak} + \sum_{i \in N^w} W_{ik} \right) \quad (10a)$$

$$\text{subject to} \quad \sum_{a \in FS(i)} v_{ak} = \sum_{a \in BS(i)} v_{ak} + g_{ik}, \forall i \in N, \forall k \in D \quad (10b)$$

$$v_{ak} \leq f_a W_{ik}, \forall a \in FS(i) : a \in A_T, \forall i \in N^w, \forall k \in D \quad (10c)$$

$$v_{ak} \leq \mathcal{A}_{Z(i)} \mathcal{V}_{Z(i)} W_{ik}, \forall a \in FS(i) : a \in A_R, \forall i \in N^w, \forall k \in D \quad (10d)$$

$$v_{ak} \geq 0, \forall a \in A, \forall k \in D \quad (10e)$$

292 The assignment program (10) minimizes the total expected link costs and wait time at waiting  
 293 nodes experienced by the passengers in a multimodal network subject to the flow conservation  
 294 constraint at each node (10b), flow proportion constraints (10c)-(10d), and the non-negativity and  
 295 binary constraints (10e). The flow proportion constraints uses the probability of selecting an option  
 296  $a \in FS(i)$  (if that option is a part of the strategy of the passengers traveling to destination  $k \in D$ )  
 297 and multiplies it with the number of passengers waiting at that node. Note that the probability of  
 298 selecting an option (MoD or transit line) is calculated in Proposition 2.

#### 299 4. Design of an integrated MoD and transit system

300 In this section, we present an optimization model incorporating the assignment program pro-  
 301 posed in previous section for the design of an integrated MoD and transit system. The optimization  
 302 program is formalized as a Mixed Integer Non-linear Program (MINLP). In this model, we deter-  
 303 mine which transit routes to keep operating among the current transit routes in the city network,  
 304 decide the optimal frequency of those operating routes, and finally, determine the fleet size of  
 305 vehicles required to provide MoD service in various zones. Note that one can also include new  
 306 candidate transit routes as part of the design plan. The sets, parameters, and decision variables  
 307 for the optimization model are summarized in Table 1.

308

309 The design of an integrated transit and MoD system should consider both passenger and oper-  
 310 ator perspectives. The operator's perspective is to provide the service at minimum cost, and the  
 311 passengers' perspective is to minimize the overall cost of travel (including travel time, wait time, and

Table 1: Sets, decision variables and parameters used in the design model

---

<u>Sets</u>	
$\mathfrak{B}$	$\triangleq$ Set of binary values
$L$	$\triangleq$ Set of candidate transit lines
$\Theta = \{2, 3, 4, 6, 12\}$	$\triangleq$ Set of possible frequencies of a line (buses/hr)
$\Omega = \{0.01, 50, 100, 200, 500\}$	$\triangleq$ Set of possible number of vehicles deployed in a zone
<u>Parameters</u>	
$\bar{B}$	$\triangleq$ Total number of buses available
$\bar{F}$	$\triangleq$ Total number of vehicles available
<u>Decision Variables</u>	
$x_l$	$= \begin{cases} 1, & \text{if line } l \in L \text{ is decided to keep operating} \\ 0, & \text{otherwise} \end{cases}$
$y_{lf}$	$= \begin{cases} 1, & \text{if frequency } f \in \Theta \text{ is adopted for line } l \in L \\ 0, & \text{otherwise} \end{cases}$
$\mathcal{N}_{zn}$	$= \begin{cases} 1, & \text{if a fleet of size } n \in \Omega \text{ is deployed in zone } z \in Z \\ 0, & \text{otherwise} \end{cases}$
$v_{ak}$	$=$ Flow of passengers on link $a \in A$ destined to $k \in D$
$W_{ik}$	$=$ Wait time of passengers waiting at node $i \in N^w$ destined to $k \in D$

---

312 fare). Based on these perspectives, the design optimization model is presented as (11). The objec-  
 313 tive function is the sum of the total expected travel cost and wait time experienced by the passengers  
 314 in the network. The mapping  $\mathcal{B} : L \times \Theta \mapsto \mathbb{N}$  used in (11b) is defined as  $\mathcal{B}(l, f) = \left( f \times \sum_{a \in A_T^l} 2t_a \right)$ ,  
 315 which describes that the number of buses required to provide frequency  $f \in \Theta$  for a line  $l \in L$   
 316 is equal to the product of the frequency and round trip travel time. (11b) constrain the total  
 317 number of buses needed to be less than or equal to  $\bar{B}$ , which can be evaluated for a given budget.  
 318 (11c) describes the flow conservation constraints at every node for every destination. For a given  
 319 MoD and bus fleet assignment, (11d)-(11e) describe the passenger flow on each link based on the  
 320 frequency of the bus route and MoD service. A frequency value can be assigned to a route if that  
 321 route is decided to keep operating as constrained by (11f). (11g) describe that exactly one of the  
 322 fleet sizes can be adopted for each zone. (11h) constrain the required number of vehicles to be less  
 323 than or equal to  $\bar{F}$ . Finally, (11i), (11j) and (11k)-(11m) are the non-negativity constraints of the  
 324 flow, wait time being free variables, and binary constraints of design variables respectively. One  
 325 can also incorporate other constraints related to the budget of operating MoD and transit service  
 326 but for the sake of simplicity, we do not include them here.

$$\begin{aligned} \text{minimize}_{v, W, x, y, \mathcal{N}} \quad & \sum_{k \in D} \left( \sum_{a \in A} c_a v_{ak} + \sum_{i \in N^w} W_{ik} \right) \end{aligned} \quad (11a)$$

$$\text{subject to} \quad \sum_{l \in L} \sum_{f \in \Theta} \mathcal{B}(l, f) \times y_{lf} \leq \bar{B} \quad (11b)$$

$$\sum_{a \in FS(i)} v_{ak} = \sum_{a \in BS(i)} v_{ak} + g_{ik}, \forall i \in N, \forall k \in D \quad (11c)$$

$$v_{ak} \leq \left( \sum_{f \in \Theta} f y_{l(a)f} \right) W_{ik}, \forall a \in FS(i) : a \in A_T, \forall i \in N^w, \forall k \in D \quad (11d)$$

$$v_{ak} \leq \mathcal{A}_{Z(i)} \left( \sum_{n \in \Omega} n \mathcal{N}_{Z(i)n} \right) W_{ik}, \forall a \in FS(i) : a \in A_R, \forall i \in N^w, \forall k \in D \quad (11e)$$

$$\sum_{f \in \Theta} y_{lf} = x_l, \forall l \in L \quad (11f)$$

$$\sum_{n \in \Omega} \mathcal{N}_{zn} = 1, \forall z \in Z \quad (11g)$$

$$\sum_{z \in Z} \left( \sum_{n \in \Omega} n \mathcal{N}_{zn} \right) \leq \bar{F} \quad (11h)$$

$$v_{ak} \geq 0, \forall a \in A, \forall k \in D \quad (11i)$$

$$W_{ik} \text{ free}, \forall i \in N^w, \forall k \in D \quad (11j)$$

$$x_l \in \mathfrak{B}, \forall l \in L \quad (11k)$$

$$y_{lf} \in \mathfrak{B}, \forall f \in \Theta, \forall l \in L \quad (11l)$$

$$\mathcal{N}_{zn} \in \mathfrak{B}, \forall n \in \Omega, z \in Z \quad (11m)$$

The optimization program (11) is a mixed-integer non-linear program (MINLP). The non-linearity arise from the constraints (11d)-(11e). It is computationally difficult to solve this program for large instances, which can be attributed to the integer constraints (11k)-(11m) and the bilinear constraints (11d)-(11e). The bilinear constraints are particularly difficult to handle due to the non-convex nature even if the integrality constraints of the involved variables are relaxed. Fortunately, in this case, the non-convexity arises due to the product of continuous and binary variables, which can be exactly relaxed by employing McCormick relaxations. Let  $t_{faik} = y_{l(a)f} W_{ik}, \forall f \in \Theta, \forall a \in FS(i) : a \in A_T, \forall i \in N^w, \forall k \in D$  and  $\omega_{ink} = \mathcal{N}_{Z(i)n} W_{ik}, \forall n \in \Omega, \forall i \in N^w \cap N_R, \forall k \in D$ . Further, let us assume that there exists a finite upper and lower bound on the variable  $W_{ik}$ , i.e.,  $\underline{W}_{ik} \leq W_{ik} \leq \bar{W}_{ik}$ . Then,  $t_{faik}$  and  $\omega_{ink}$  can be expressed as the set of linear constraints

(12a)-(12d) and (13a)-(13d) respectively:

$$\overline{W}_{ik} - W_{ik} + t_{faik} - \overline{W}_{ik}y_{l(a)f} \geq 0 \quad (12a)$$

$$\overline{W}_{ik}y_{l(a)f} - t_{faik} \geq 0 \quad (12b)$$

$$t_{faik} - \underline{W}_{ik}y_{l(a)f} \geq 0 \quad (12c)$$

$$W_{ik} - \underline{W}_{ik} - t_{faik} + \underline{W}_{ik}y_{l(a)f} \geq 0 \quad (12d)$$

$$\overline{W}_{ik} - W_{ik} + \omega_{ink} - \overline{W}_{ik}\mathcal{N}_{Z(i)n} \geq 0 \quad (13a)$$

$$\overline{W}_{ik}\mathcal{N}_{Z(i)n} - \omega_{ink} \geq 0 \quad (13b)$$

$$\omega_{ink} - \underline{W}_{ik}\mathcal{N}_{Z(i)n} \geq 0 \quad (13c)$$

$$W_{ik} - \underline{W}_{ik} - \omega_{ink} + \underline{W}_{ik}\mathcal{N}_{Z(i)n} \geq 0 \quad (13d)$$

## 327 5. Solution methodology

328 After relaxing the bilinear constraints (11d)-(11e), the resulting model is a Mixed Integer Linear  
 329 Program (MILP). The program is still difficult to solve efficiently for large instances. However, the  
 330 structure of the problem allows us to use decomposition techniques such as Benders decomposition  
 331 to efficiently solve it. In this section, we present the details of the Benders reformulation for this  
 332 problem, along with the proposed algorithmic enhancements.

### 333 5.1. Benders Reformulation

334 Benders decomposition (Geoffrion 1972) is an elegant way of solving a large scale MILP by iter-  
 335 atively solving two simpler subproblems: the relaxed master problem (RMP), which is a relaxation  
 336 of the original problem and a subproblem (SP) which provides inequalities/cuts to strengthen the  
 337 RMP. The subproblem should possess strong duality properties. Let us consider the network design  
 338 problem described in the previous section. For a given feasible value of design decision variables  
 339  $\hat{x}, \hat{y}, \hat{\mathcal{N}}$  and with  $\underline{W}_{ik} = 0$  (wait time cannot be negative), we can rewrite the original problem as  
 340 a *Benders subproblem* (14).

$$z^{SP}(\hat{x}, \hat{y}, \hat{\mathcal{N}}) = \min_{v, W, \omega, t} \sum_{k \in D} \left( \sum_{a \in A} c_a v_{ak} + \sum_{i \in N^w} W_{ik} \right) \quad (14a)$$

$$\text{subject to} \quad \sum_{a \in FS(i)} v_{ak} = \sum_{a \in BS(i)} v_{ak} + g_{ik}, \forall i \in N, \forall k \in D \quad (14b)$$

$$v_{ak} \leq \left( \sum_{f \in \Theta} f t_{faik} \right), \forall a \in FS(i) : a \in A_T, \forall i \in N^w, \forall k \in D \quad (14c)$$

$$W_{ik} - t_{faik} \leq \bar{W}_{ik}(1 - \hat{y}_{l(a)f}), \forall f \in \Theta, \forall a \in FS(i) : a \in A_T, \forall i \in N^w, \forall k \in D \quad (14d)$$

$$t_{faik} \leq \bar{W}_{ik} \hat{y}_{l(a)f}, \forall f \in \Theta, \forall a \in FS(i) : a \in A_T, \forall i \in N^w, \forall k \in D \quad (14e)$$

$$W_{ik} - t_{faik} \geq 0, \forall f \in \Theta, \forall a \in FS(i) : a \in A_T, \forall i \in N^w, \forall k \in D \quad (14f)$$

$$v_{ak} \leq \mathcal{A}_{Z(i)} \left( \sum_{n \in \Omega} n \omega_{ink} \right), \forall a \in FS(i) : a \in A_R, \forall i \in N^w, \forall k \in D \quad (14g)$$

$$W_{ik} - \omega_{ink} \leq \bar{W}_{ik}(1 - \hat{\mathcal{N}}_{Z(i)n}), \forall n \in \Omega, \forall i \in N^w \cap N_R, \forall k \in D \quad (14h)$$

$$\omega_{ink} \leq \bar{W}_{ik} \hat{\mathcal{N}}_{Z(i)n}, \forall n \in \Omega, \forall i \in N^w \cap N_R, \forall k \in D \quad (14i)$$

$$W_{ik} - \omega_{ink} \geq 0, \forall n \in \Omega, \forall i \in N^w \cap N_R, \forall k \in D \quad (14j)$$

$$v_{ak} \geq 0, \forall a \in A, \forall k \in D \quad (14k)$$

$$t_{faik} \geq 0, \forall f \in \Theta, \forall a \in FS(i) : a \in A_T, \forall i \in N^w, \forall k \in D \quad (14l)$$

$$\omega_{ink} \geq 0, \forall n \in \Omega, \forall i \in N^w \cap N_R, \forall k \in D \quad (14m)$$

341 Let  $\mathcal{X}^{SP} = \{(v, W, \omega, t) : (14b) - (14m)\}$  be the feasible region of the Benders subproblem (14).  
 342 Further, let us denote  $\mathcal{X}^{MA} = \{(v, W) : (10b) - (10e)\}$  as the feasible region of the multimodal  
 343 assignment linear program. We can show the following result:

**Proposition 3.** *The projection of the feasible region of the subproblem (14) on to the space of  $v$  and  $W$  is same as the feasible region of the multimodal assignment problem (10) i.e.,*

$$\text{proj}_{v, W} \mathcal{X}^{SP} = \mathcal{X}^{MA}$$

344 *Proof.* See Appendix A. □

345 Proposition 3 shows that one can use the efficient Spiess and Florian 1989's primal-dual algo-  
 346 rithm designed for the transit assignment problem to solve the current Benders subproblem. To  
 347 speed up the process of Benders decomposition by avoiding feasibility cuts, we need to put some  
 348 restrictions so that the subproblem (14) is always feasible.

349 **Proposition 4.** *Given that  $0 \notin \Omega$  and  $G_R(N_R, A_R)$  is connected, then  $\mathcal{X}^{SP}$  is non-empty for any  
 350 given feasible value of  $\hat{x}, \hat{y}, \hat{\mathcal{N}}$ .*



351 *Proof.* See Appendix A. □

352 Proposition 4 makes the Benders subproblem feasible for any feasible value of  $\hat{x}, \hat{y}, \hat{\mathcal{N}}$ . This is  
 353 an important result to make the Benders decomposition implementation faster.

354

355 Let  $\{\mu_{ik}\}, \{\lambda_{aik}^1\}, \{\lambda_{faik}^2\}, \{\lambda_{faik}^3\}, \{\lambda_{faik}^4\}, \{\lambda_{aik}^5\}, \{\lambda_{nik}^6\}, \{\lambda_{nik}^7\}$ , and  $\{\lambda_{nik}^8\}$  be the dual  
 356 variables associated with the constraints (14b) -(14j) respectively. Then, the dual of the subproblem  
 357 DSP can be stated as below:

$$z^{DSP}(\hat{x}, \hat{y}, \hat{\mathcal{N}}) = \max_{\mu, \lambda} \sum_{k \in D} \left[ \sum_{i \in N} \mu_{ik} g_{ik} + \sum_{i \in N^w} \sum_{a \in FS(i): a \in A_T} \sum_{f \in \Theta} (\bar{W}_{ik} (1 - \hat{y}_{l(a)f}) \lambda_{faik}^2 \right. \\ \left. + \bar{W}_{ik} \hat{y}_{l(a)f} \lambda_{faik}^3) \right) + \sum_{i \in N^w \cap N_R} \sum_{n \in \Omega} (\bar{W}_{ik} (1 - \hat{\mathcal{N}}_{Z(i)n}) \lambda_{nik}^6 \\ \left. + \bar{W}_{ik} \hat{\mathcal{N}}_{Z(i)n} \lambda_{nik}^7) \right] \quad (15a)$$

$$\text{subject to} \quad \mu_{ik} - \mu_{jk} + \lambda_{aik}^1 + \lambda_{aik}^5 \leq c_a, \forall a = (i, j) \in A, \forall k \in D \quad (15b)$$

$$- \sum_{f \in \Theta} \sum_{\substack{a \in FS(i): \\ a \in A_T}} (\lambda_{faik}^2 + \lambda_{faik}^4) + \sum_{n \in \Omega} (\lambda_{nik}^6 + \lambda_{nik}^8) = 1, \forall i \in N^w, \forall k \in D \\ (15c)$$

$$- f \lambda_{aik}^1 - \lambda_{faik}^2 + \lambda_{faik}^3 - \lambda_{faik}^4 \leq 0, \forall f \in \Theta, \forall a \in FS(i) : a \in A_T, \forall i \in N^w, \forall k \in D \quad (15d)$$

$$- n \lambda_{aik}^5 - \lambda_{nik}^6 + \lambda_{nik}^7 - \lambda_{nik}^8 \leq 0, \forall n \in \Omega, \forall i \in N^w \cap N_R, \forall k \in D \quad (15e)$$

$$\lambda_{aik}^1, \lambda_{aik}^5 \leq 0, \forall a \in FS(i), \forall i \in N^w, \forall k \in D \quad (15f)$$

$$\lambda_{faik}^2, \lambda_{faik}^3 \leq 0, \lambda_{faik}^4 \geq 0, \forall f \in \Theta, \forall a \in FS(i) : a \in A_T, \forall i \in N^w, \forall k \in D \\ (15g)$$

$$\lambda_{nik}^6, \lambda_{nik}^7 \leq 0, \lambda_{nik}^8 \geq 0, \forall n \in \Omega, \forall i \in N^w \cap N_R, \forall k \in D \quad (15h)$$

358 Let us denote the feasible region of DSP as  $\Pi = \{(\mu, \lambda^1, \lambda^2, \lambda^3, \lambda^4, \lambda^5, \lambda^6, \lambda^7, \lambda^8) : (15b) - (15h)\}$ .  
 359 Note that  $\Pi$  does not depend on the value of  $x, y, \mathcal{N}$ . From Proposition 4, we know that SP is always  
 360 feasible for any given feasible value of  $(\hat{x}, \hat{y}, \hat{\mathcal{N}})$ , then by linear programming duality, DSP should be  
 361 bounded. The implication is that the polyhedron describing  $\Pi$  is bounded and can be described as  
 362 the convex hull of a set of extreme points only (from Minkowski-Weyl's theorem on characterization  
 363 of polyhedra (Conforti et al. 2014, Chapter 3)). Let  $\{(\mu^\pi, (\lambda^1)^\pi, (\lambda^2)^\pi, (\lambda^3)^\pi, (\lambda^4)^\pi, (\lambda^5)^\pi, (\lambda^6)^\pi, (\lambda^7)^\pi, (\lambda^8)^\pi)\}_{\pi \in \mathcal{K}}$   
 364 be the set of extreme points of polytope  $\Pi$ , where  $\mathcal{K}$  represents the set of indices of extreme points.  
 365 By applying an outer linearization procedure to the inner (sub) problem of the original problem,  
 366 we can restate it as (16), which is referred to as the *Benders Master problem* (MP).

**Theorem 1.** (Benders 1962) *The problem (11) can be reformulated as below:*

$$\begin{array}{ll} \text{minimize} & \eta \\ & x, y, \mathcal{N}, \eta \end{array} \quad (16a)$$

$$\text{subject to} \quad \sum_{l \in L} \sum_{f \in \Theta} \mathcal{B}(l, f) \times y_{lf} \leq \bar{B} \quad (16b)$$

$$\sum_{f \in \Theta} y_{lf} = x_l, \forall l \in L \quad (16c)$$

$$\sum_{n \in \Omega} \mathcal{N}_{zn} = 1, \forall z \in Z \quad (16d)$$

$$\sum_{z \in Z} \left( \sum_{n \in \Omega} n \mathcal{N}_{zn} \right) \leq \bar{F} \quad (16e)$$

$$\begin{aligned} \eta \geq \sum_{k \in D} \left[ \sum_{i \in N} (\mu_{ik})^\pi g_{ik} + \sum_{i \in N^w} \sum_{a \in FS(i): a \in A_T} \sum_{f \in \Theta} (\bar{W}_{ik} (1 - \hat{y}_{l(a)f}) (\lambda_{f aik}^2)^\pi) \right. \\ \left. + \bar{W}_{ik} \hat{y}_{l(a)f} (\lambda_{f aik}^3)^\pi \right) + \sum_{i \in N^w \cap N_R} \sum_{n \in \Omega} \left( \bar{W}_{ik} (1 - \hat{\mathcal{N}}_{Z(i)n}) (\lambda_{nik}^6)^\pi \right. \\ \left. + \bar{W}_{ik} \hat{\mathcal{N}}_{Z(i)n} (\lambda_{nik}^7)^\pi \right) \right], \forall \pi \in \mathcal{K} \end{aligned} \quad (16f)$$

$$x_l \in \mathfrak{B}, \forall l \in L \quad (16g)$$

$$y_{lf} \in \mathfrak{B}, \forall f \in \Theta, \forall l \in L \quad (16h)$$

$$\mathcal{N}_{in} \in \mathfrak{B}, \forall n \in \Omega, i \in Z \quad (16i)$$

367 *Proof.* See Benders 1962. □

## 368 5.2. Classic Benders decomposition implementation

369 The issue with the Benders reformulation is that there could be a large number of extreme  
370 points of the polyhedron associated with the feasible region of DSP, therefore, one applies an  
371 iterative process of solving two problems, namely, the relaxed master problem (RMP) and the  
372 subproblem (SP) repeatedly. The relaxed master problem is the master problem with constraints  
373 (16f) being defined only for a subset of extreme points, i.e.,  $\mathcal{K}' \subset \mathcal{K}$ . The overall implementation of  
374 the classic Benders Decomposition is summarized in Algorithm 1. We start by finding the feasible  
375 value of  $(x^0, y^0, \mathcal{N}^0)$ . This can be done by solving (16) without (16f) and including a constraint  
376  $\eta \geq 0$ . Then, in each iteration  $t$ , the algorithm solves RMP with the given set of extreme points  
377 and then SP with the current value of  $(x^t, y^t, \mathcal{N}^t)$ . Since RMP is relaxation and SP is solved for a  
378 feasible value  $(x^t, y^t, \mathcal{N}^t)$ , they provide a lower bound and upper bound respectively to the original  
379 problem. The subproblem also provides inequalities (optimality cuts) to strengthen the formulation  
380 of RMP in each iteration. Thus, it is guaranteed to have non-decreasing lower bounds. In our case,  
381 there are no feasibility cuts since our subproblem is always feasible (Proposition 4). The algorithm  
382 terminates when both the upper bound and lower bound are close to each other.

---

**Algorithm 1** Classic Benders decomposition implementation
 

---

- 1: (*Initialize*) Let  $t = 0, UB = -\infty, LB = \infty, \mathcal{K}' = \phi$ . Assume an initial feasible value  $(x^0, y^0, \mathcal{N}^0)$ .  
Solve the SP (14), obtain the optimal dual solution and append that to set  $\mathcal{K}'$ .
  - 2: **while**  $UB - LB > \epsilon$  **do**  $\triangleright \epsilon$  is the tolerance parameter
  - 3:   Set  $t = t + 1$ . Solve RMP (16) and obtain its optimal solution  $(x^t, y^t, \mathcal{N}^t)$ .
  - 4:   Set  $LB = \eta$
  - 5:   Solve SP (14) for  $(x^t, y^t, \mathcal{N}^t)$ , obtain dual solutions and append that to  $\mathcal{K}'$ .
  - 6:   Set  $UB = \sum_{k \in D} (\sum_{a \in A} c_a v_{ak}^t + \sum_{i \in N^w} W_{ik}^t)$
- 

 383 *5.3. Enhanced Benders decomposition implementation*

 384     The classic Benders decomposition may take prohibitive computational effort to converge, thus  
 385 making it difficult to solve the problem for large instances. The slow convergence can be attributed  
 386 to the low strength of the optimality cuts, degeneracy in the subproblem, no guarantee of non-  
 387 decreasing upper bounds in each iteration, or not formulating the problem "properly" (Saharidis  
 388 and Ierapetritou 2010, Tang et al. 2013, Magnanti and Wong 1981). To accelerate the Benders  
 389 decomposition algorithm, we make use of several enhancements that are described below:

 390 *5.3.1. Use of multiple cuts via disaggregated cuts*

 391     For this design problem, we can further utilize the decomposable structure of the Benders sub-  
 392 problem (11) as it is decomposable for each destination  $k \in D$ . That is, we can solve several  
 393 (smaller) subproblems and generate multiple optimality cuts for the master problem. The disag-  
 394 gregated cuts have a higher probability of finding facet-defining inequalities characterizing  $\Pi$ . For  
 395 this purpose, we modify RMP to allow for the disaggregated cuts as (17):

$$\underset{x, y, \mathcal{N}, \eta}{\text{minimize}} \quad \sum_{k \in D} \eta_k \tag{17a}$$

$$\text{subject to} \quad (16b) - (16e) \tag{17b}$$

$$\eta_k \geq \left[ \sum_{i \in N} (\mu_{ik})^\pi g_{ik} + \sum_{i \in N^w} \sum_{a \in FS(i): a \in A_T} \sum_{f \in \Theta} (\bar{W}_{ik} (1 - \hat{y}_{l(a)f}) (\lambda_{faik}^2)^\pi \right. \\ \left. + \bar{W}_{ik} \hat{y}_{l(a)f} (\lambda_{faik}^3)^\pi) \right] + \sum_{i \in N^w \cap N_R} \sum_{n \in \Omega} \left( \bar{W}_{ik} (1 - \hat{\mathcal{N}}_{Z(i)n}) (\lambda_{nik}^6)^\pi \right. \\ \left. + \bar{W}_{ik} \hat{\mathcal{N}}_{Z(i)n} (\lambda_{nik}^7)^\pi \right), \forall \pi \in \mathcal{K}_k, \forall k \in D \tag{17c}$$

$$(16g) - (16i) \tag{17d}$$

 396     Note that by adding the disaggregated cuts for every destination, we can get back the optimality  
 397 cuts defined in the classic Benders relaxed master problem.

398 *5.3.2. Use of multiple cuts via multiple solutions*

399 To further improve the convergence of the algorithm, Beheshti Asl and MirHassani 2019 used  
 400 a strategy known as multiple cuts via multiple solutions. When solving the RMP, any commercial  
 401 solver such as AIMMS or GUROBI can be asked to generate multiple solutions of an integer program  
 402 (optimal as well as suboptimal) by using `pool solution option`. These multiple solutions can be  
 403 used to generate multiple classic (16f) or disaggregated cuts (17c) to be added in next iteration of  
 404 RMP. This strategy is expected to decrease the overall iterations and possibly the solution time of  
 405 the algorithm.

406 *5.3.3. Use of clique/cover cuts*

407 Due to the limited availability of bus and vehicle fleet, one can use the clique/cover cuts to  
 408 tighten the feasible region of the master problem.

409 **Proposition 5.** *For every  $n \in \Omega$ , if  $\lfloor \frac{\bar{F}}{n} \rfloor < |Z|$  then the clique inequality  $\sum_{z \in Z} \mathcal{N}_{zn} \leq \lfloor \frac{\bar{F}}{n} \rfloor$  is valid*  
 410 *for (11).*

411 *Proof.* See Appendix A. □

412 If for any  $n \in \Omega$ , we have  $\lfloor \frac{\bar{F}}{n} \rfloor > |Z|$ , then the inequality  $\sum_{z \in Z} \mathcal{N}_{zn} \leq \lfloor \frac{\bar{F}}{n} \rfloor$  will be redundant  
 413 and therefore, we do not add it to the model.

414

415 The inequality which constrain the number of buses (11b) is a Knapsack constraint. A set  
 416  $C \subseteq L \times \Theta$  is a *cover* for inequality (11b) if  $\sum_{(l,f) \in C} \mathcal{B}(l,f) > \bar{B}$  and it is *minimal cover* if  
 417  $\sum_{(l,f) \in C \setminus \{(l',f')\}} \mathcal{B}(l,f) \leq \bar{B}$ , for all  $(l',f') \in C$

418 **Proposition 6.** *For any minimal cover  $C \subseteq L \times \Theta$ , the inequality  $\sum_{(l,f) \in C} y_{lf} \leq |C| - 1$  is valid*  
 419 *for (11).*

420 *Proof.* See Appendix A. □

421 To generate some of the minimal cover cuts, one can use the heuristic given in Algorithm 2. In  
 422 this algorithm, for each frequency  $f \in \Theta$ , we keep the list of lines  $G$  for which the number of buses  
 423 required to provide the frequency  $f$  does not exceed  $\bar{B}$ . Then, any line which is not in  $G$ , along  
 424 with  $G$  forms a minimal cover.

---

**Algorithm 2** Cover cut generation heuristic

---

```
1: procedure
2:   Compute the value of mapping  $\mathcal{B}(l, f)$  for all  $(l, f) \in L \times \Theta$ .
3:    $CC \leftarrow \phi$ 
4:   for  $f \in \Theta$  do
5:      $G \leftarrow []$ ;  $temp \leftarrow 0$ 
6:     for  $l \in L : \mathcal{B}(l, f)$  in an ascending order do
7:        $temp = temp + \mathcal{B}(l, f)$ 
8:       if  $temp \leq \bar{B}$  then
9:         append  $(l, f)$  to  $G$ 
10:      else
11:        break
12:      for  $l \in L \setminus G$  do
13:         $C \leftarrow G \cup \{(l, f)\}$ 
14:      append  $C$  to  $CC$ 
return  $CC$ 
```

---

425 Furthermore, one can use other efficient techniques to produce maximal clique or minimal cover  
426 cuts for the problem.

#### 427 5.3.4. Other recommendations

428 One of the problems with the Benders subproblem (14) is that it assumes the value of  $\bar{W}_{ik}$  as  
429 a given upper bound. The value of  $\bar{W}_{ik}$  is a big-M introduced to relax the non-linearity in the  
430 original model. If the value of the big-M is not chosen properly, then one can face serious issues  
431 with the convergence of the algorithm. For example, choosing  $\bar{W}_{ik} < W_{ik}$  can make the subproblem  
432 infeasible, and choosing  $\bar{W}_{ik}$  too high would generate weak optimality cuts, which would increase  
433 the computational time of the algorithm. One way to avoid this issue is to solve the assignment  
434 problem (10) for given design variables  $(x, y, \mathcal{N})$  and compute the optimal value of  $W_{ik}$  and use  
435 that as an upper bound. Further improvements in the Benders decomposition method can involve  
436 the use of *pareto-optimal* cuts proposed by Magnanti and Wong 1981. They help in avoiding the  
437 generation of multiple optimality cuts for a degenerate subproblem. We tried this strategy, however,  
438 we did not find any significant improvement in the solution time using these cuts, therefore, we  
439 do not discuss it here. Finally, when RMP is loaded with a large number of cuts we recommend  
440 removing the non-active cuts from the model by checking the slack value. There is no guarantee  
441 that they will not be generated again, but it will be faster to solve the RMP. The overall steps of  
442 the Benders implementation with possible acceleration techniques are summarized in Algorithm 3.

---

**Algorithm 3** Enhanced Benders decomposition implementation

---

- 1: (*Initialize*) Let  $t = 0, UB = -\infty, LB = \infty, \mathcal{K}'_k = \phi, \forall k \in D$ .
  - 2: Prepare the master problem with clique and cover inequalities.
  - 3: Assume an initial feasible value  $(x^0, y^0, \mathcal{N}^0)$ . Solve the SP (14), obtain the optimal dual solutions and append that to the set  $\mathcal{K}'_k, \forall k \in D$ .
  - 4: **while**  $UB - LB > \epsilon$  **do**  $\triangleright \epsilon$  is the tolerance parameter
  - 5:     Set  $t = t + 1$ . Solve RMP (16), obtain its optimal solution  $(x_0^t, y_0^t, \mathcal{N}_0^t)$  and other optimal/-suboptimal solutions  $\{(x_s^t, y_s^t, \mathcal{N}_s^t)\}_{1 \leq s \leq l}$ , where  $l$  is specified by the user.
  - 6:     Set  $LB = \sum_{k \in D} \eta_k$
  - 7:     **for**  $s = 0, 1, \dots, l$  **do**
  - 8:         Solve SP (14) for  $(x_s^t, y_s^t, \mathcal{N}_s^t)$ , obtain dual solution and append that to  $\mathcal{K}'_k, \forall k \in D$ .
  - 9:     Set  $UB = \sum_{k \in D} (\sum_{a \in A} c_a v_{ak}^t + \sum_{i \in N^w} W_{ik}^t)$
- 

## 443 6. Computational results

444     In this section, we present the computational study based on the model (11), (16), and accelera-  
445     tion techniques presented in §5.3. We start by describing the details of the experiment used to show  
446     the application of the proposed method. Then, we present the details of the network design results  
447     in §6.2, which is followed by the comparison of the computational performance of the solver, the  
448     classic Benders implementation, and the enhanced Benders techniques described in §6.3. Finally,  
449     we discuss the results of the sensitivity analysis on two important parameters in the model, namely,  
450     the available fleet of buses  $\bar{B}$  and vehicles  $\bar{F}$  in §6.4, which is followed by the comparison of the  
451     performance of optimized existing transit system and proposed integrated system in §6.5.

### 452 6.1. Experiment details

453     The computational experiments are based on the Sioux Falls road and transit network. The road  
454     network has 24 nodes, whereas the static transit network has 384 stops. A walking distance of 0.5  
455     miles is used to create walking links. An illustration of the two networks is shown in Figure 2 and the  
456     number of different types of links in the network is given in Table 2. There are 12 candidate transit  
457     routes in the transit network. We consider the set of possible frequencies as  $\Theta = \{2, 3, 4, 6, 12\}$   
458     buses/hr to be assigned to any candidate transit route and possible vehicle fleet size to be assigned  
459     to any zone as  $\Omega = \{0.01, 50, 100, 200, 500\}$ . The vehicle fleet size value 0.01 is a dummy element to  
460     represent that no vehicles are assigned in a zone and that zone can be served by transit service only.  
461     A time-based fare of \$0.21/ min and a base fare of \$0.8 is assumed for the MoD service, whereas  
462     the transit fare is assumed to be a fixed value of \$2. To convert the monetary costs into time units,  
463     the value of travel time equal to 23\$/hr is used. The value of parameter  $\mathcal{A}$  used in the wait time  
464     computations of MoD service is assumed to be equal to 0.0017 for all the zones (Yin 2019). The  
465     available number of buses  $\bar{B}$  and vehicles  $\bar{F}$  are assumed to be 70 and 3,000 respectively. There are  
466     576 O-D pairs in the network with a total number of trips equal to 36,060. All implementations

Table 2: Number of different types of links in the Sioux Falls multimodal network

Link type	Number of links
Access ( $A^a$ )	243
Egress ( $A^e$ )	243
Road ( $A_R$ )	76
Transit ( $A_T$ )	398
Transit transfer ( $A_T^{tr}$ )	368
Mode transfer ( $A^m$ )	152

467 are coded in Python 3.8 using Gurobi 9.0.1 as the optimization solver. The tests were executed  
 468 on Intel(R) i7-7700 CPU running at 3.6 GHz with 32 GB RAM under a Windows operating system.

469

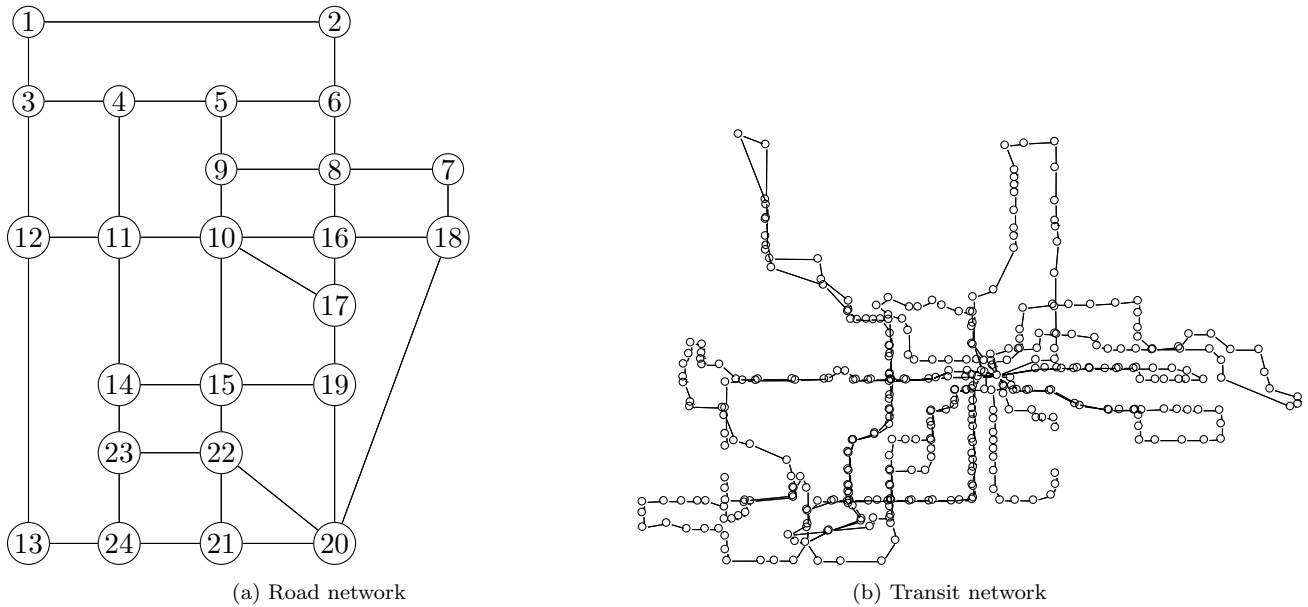


Figure 2: Sioux Falls network

470 *6.2. Network design results*

471 We solve the network design problem (11) for the instance explained in §6.1. The selected  
 472 transit routes with their optimal frequency are given in Table 3. Out of 12 candidate routes, 6  
 473 routes are decided to keep operating. The transit network with active and inactive routes is shown  
 474 in Figure 3. We observe that most of the routes are located in the central region of the network.  
 475 All the routes have been assigned the highest frequency i.e., 12 buses/hr, except route 8, which  
 476 has been assigned a frequency of 3 buses/hr. To provide this service, 69 buses are required. The  
 477 average number of vehicles deployed in each zone is given in Table 4. In the optimal allocation of  
 478 vehicles, it is decided not to deploy any vehicles in 10 zones out of 24 zones. Most of the zones have  
 479 been allocated 200 vehicles providing an average wait time of 3 minutes. We further observe that

480 the vehicles are deployed in the outskirts zones of the network where transit routes are not located.

481

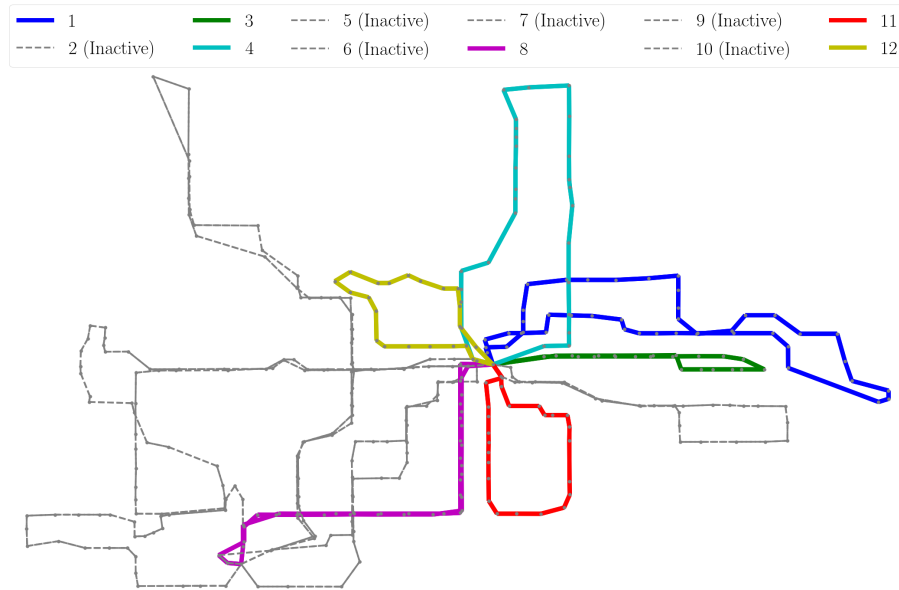


Figure 3: Transit routes (inactive routes are shown by dashed gray color)

Table 3: Selected transit routes with their optimal frequency

Route	Located?	Optimal frequency (buses/hr)	Average wait time (min)
1	Yes	12	5
2	No	-	-
3	Yes	12	5
4	Yes	12	5
5	No	-	-
6	No	-	-
7	No	-	-
8	Yes	3	20
9	No	-	-
10	No	-	-
11	Yes	12	5
12	Yes	12	5

482 The total time spent in the system is equal to 11,301 passenger-hours including 8,673 passenger-  
 483 hours of travel time on various links, 1,881 passenger-hours of wait time spent on the transit network,  
 484 and 747 passenger-hours of wait time spent on the road network. We found that more passengers



Table 4: vehicle allocation to different zones

Zone	Vehicles	Avg. Wait time (min)	Zone	Vehicles	Avg. Wait time (min)
1	200	3	13	200	3
2	100	6	14	200	3
3	200	3	15	200	3
4	200	3	16	-	-
5	-	-	17	-	-
6	-	-	18	200	3
7	200	3	19	200	3
8	-	-	20	200	3
9	-	-	21	-	-
10	-	-	22	-	-
11	200	3	23	-	-
12	500	1.2	24	200	3

485 take transit than MoD service. The share of passengers using the road, transit, and multimodal  
 486 service are 23 %, 61 %, and 16 % respectively. The passenger flow on various links and wait time  
 487 on various nodes of the road and transit networks (resp.) are visualized in Figure 4(a) and (b)  
 488 respectively. We observe that most of the passenger trips in the central zones are made using  
 489 transit network, whereas the trips on the outskirts of the network are made using both MoD and  
 490 multimodal service. The figures further show that the congestion in the central zones is significantly  
 491 improved with the resulting network design.

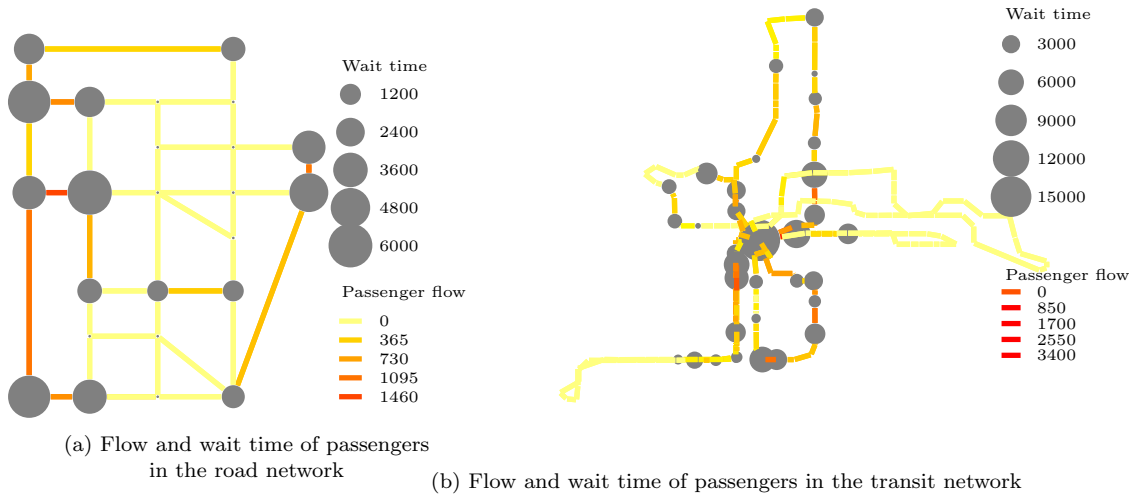


Figure 4: Flow and wait time (pass-min) of passengers in the network

492 *6.3. Computational performance*

493 In this section, we compare the computational performance of various models and implementa-  
 494 tion techniques. We consider the following approaches to compare:

- 495 1. Solving model (11) using Gurobi solver

Table 5: Computational performance

Method	Iterations	Computational time (s)	Gap (%)
Gurobi bilinear	-	Timed out*	13.3
Gurobi	-	Timed out*	0.62
Classic	734	Timed out*	0.16
Classic + Clique/Cover	510	7,440	0
Classic + Multiple	500	6,524	0
Classic + Clique/Cover + Multiple	423	5,566	0
Disaggregate	31	381	0
Disaggregate + Clique/Cover	30	347	0
Disaggregate + Multiple	28	535	0
Disaggregate + Multiple + Clique/Cover	27	498	0

\*Note: Maximum time limit = 3 hours

- 496 2. Solving model (16) using Gurobi solver
- 497 3. Solving model (16) using classic Benders decomposition (Algorithm 1)
- 498 4. Solving model (16) using Benders decomposition with clique/cover cuts (§5.3.3)
- 499 5. Solving model (16) using Benders decomposition with multiple cuts via multiple solutions  
500 (§5.3.2)
- 501 6. Solving model (16) using Benders decomposition with both clique/cover and multiple cuts  
502 via multiple solutions
- 503 7. Solving model (16) using Benders decomposition with disaggregated cuts (§5.3.1)
- 504 8. Solving model (16) using Benders decomposition with disaggregated and clique/cover cuts
- 505 9. Solving model (16) using Benders decomposition with disaggregated and multiple cuts via  
506 multiple solutions
- 507 10. Solving model (16) using Benders decomposition with disaggregated, clique/cover, and mul-  
508 tiple cuts via multiple solutions

509 To solve the bilinear model (11), we set the Gurobi parameter `NonConvex` = 2. For Benders de-  
510 composition with multiple cuts via multiple solutions, we set the Gurobi parameters `PoolSolutions`  
511 = 2, `PoolGap` = 0.01, `PoolSearchMode` = 2. For all above tests, the maximum time limit was set  
512 to 3 hours.

513

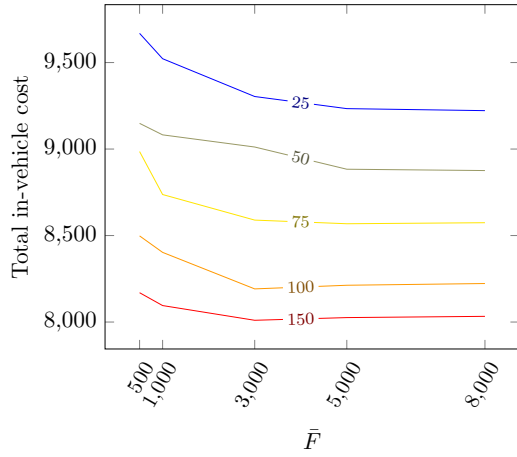
514 The computational performance of every method is shown in Table 5. The iterations are counted  
515 as the number of times RMP is solved, the computational time is recorded in seconds, and Gap is  
516 defined as  $(UB - LB) * 100 / UB$ . The bilinear model (11) is hard to solve, and Gurobi took 3 hours

517 to reach the optimality gap of 13.3 %. The rest of the results are discussed for the optimization  
 518 model (16). Other than Gurobi and classic Benders decomposition, all the methods coverage to the  
 519 optimal solution. Gurobi and classic Benders decomposition reached an optimality gap of 0.62%  
 520 and 0.16% respectively. This means both methods reached very close to the optimal solution in  
 521 3 hours. The hybrid approach of classic Benders decomposition with both clique/cover cuts and  
 522 multiple cuts via multiple solutions outperforms the classic Benders decomposition with clique/-  
 523 cover cuts or multiple cuts via multiple solutions only. The disaggregated Benders decomposition  
 524 is computationally more efficient than any classic Benders approach with cut improvements. The  
 525 disaggregated cuts with other cuts show further improvement in the solution time and the number  
 526 of iterations to converge to the optimal solution. The Benders decomposition using disaggregated,  
 527 clique/cover, and multiple cuts via multiple solutions outperforms other methods in terms of the  
 528 number of iterations to converge to an optimal solution, whereas Benders decomposition with dis-  
 529 aggregated and clique/cover cuts outperform other methods in terms of computational time. This  
 530 may be because the multiple cuts are generated by solving several subproblems, which takes more  
 531 computational time, but the generated cuts may not be as effective. Overall, the experiments  
 532 performed for this section show that the computational methods presented in this study are quite  
 533 efficient in solving the current problem exactly.

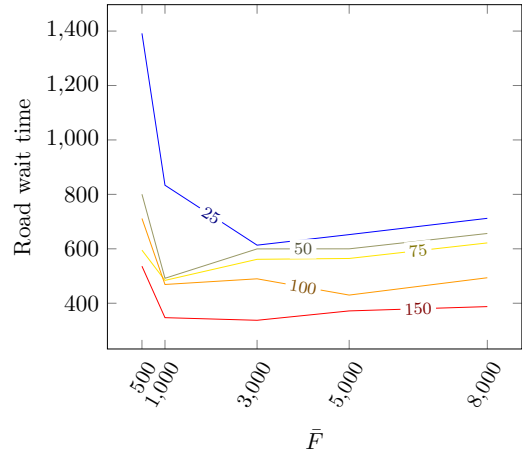
#### 534 6.4. Sensitivity analysis on parameters

535 The availability of buses and vehicles can result in different network design results. Hence, we  
 536 choose to perform a sensitivity analysis on the available bus fleet  $\bar{B}$  and vehicle fleet  $\bar{F}$ . We solve  
 537 the model (16) with varying bus fleet size of 25, 50, 75, 100, and 150 and varying vehicle fleet  
 538 size of 500, 1000, 3000, 5000, 8000. Figure 5 and 6 show the sensitivity analysis results based on  
 539 contour plots. The x-axis shows the varying vehicle fleet sizes, and contours represent varying bus  
 540 fleet sizes. Figure 5(a), (b), (c), and (d) show the in-vehicle cost, average road wait time, average  
 541 transit wait time, and total expected travel cost in passenger-hours respectively. We can observe  
 542 that the in-vehicle cost decreases with the increase in the number of available vehicles. The effect  
 543 of increasing the number of buses is more than the increase in the number of vehicles. Moreover,  
 544 the in-vehicle cost is not affected by increasing the number of vehicles to more than 5,000. The  
 545 average road wait time decreases with the increase in the number of available vehicles. It also  
 546 decreases with the increase in the number of available buses due to mode shift. The passenger-  
 547 hours spent as the wait time in the transit network increases with the increase in the number of  
 548 available vehicles as well as buses. This is because more passengers take the transit mode as more  
 549 buses are made available. The overall expected travel cost also reduces with the increase in the bus  
 550 and vehicle fleet. However, the effect of an increase in the vehicle fleet size of more than 5,000 is  
 551 negligible. Figure 6 shows the mode share as a function of the available bus and vehicle fleet size.  
 552 As expected, the transit and MoD share increase with the increase in the available bus and vehicle  
 553 fleet size respectively. The share of multimodal service increases with the number of vehicles and  
 554 buses up to 5,000 and 75 respectively but declines after that. The decline in multimodal share

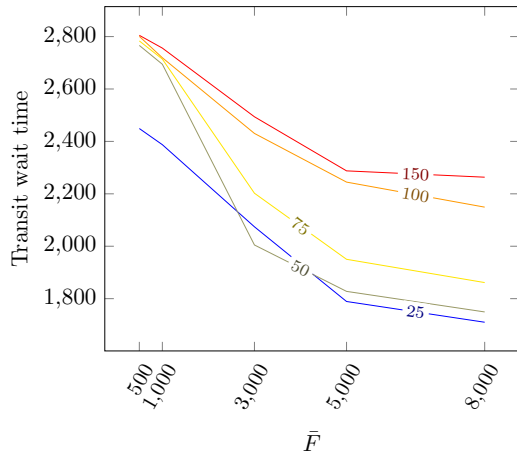
555 is because of the reduced wait time for both services, which drives passengers to use single mode  
 556 rather than multiple modes.



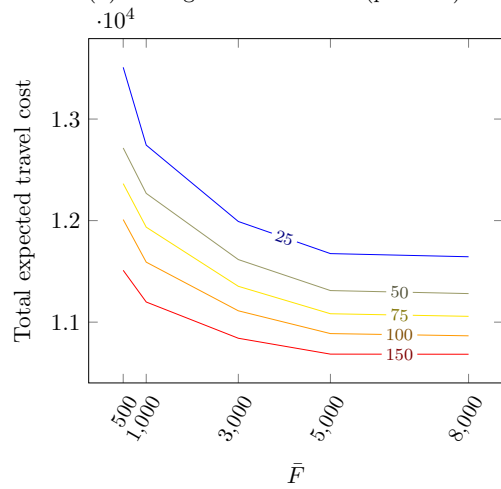
(a) In-vehicle cost (pass-hrs)



(b) Average road wait time (pass-hrs)

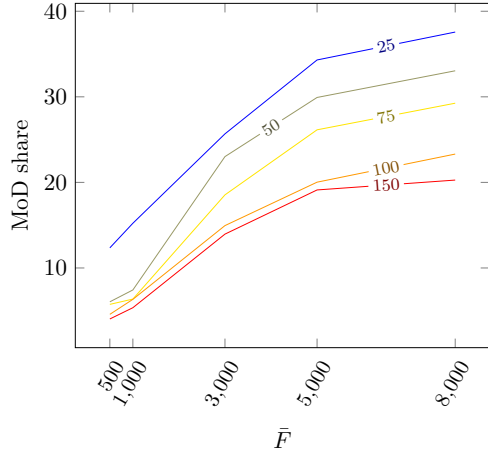


(c) Average transit wait time (pass-hrs)

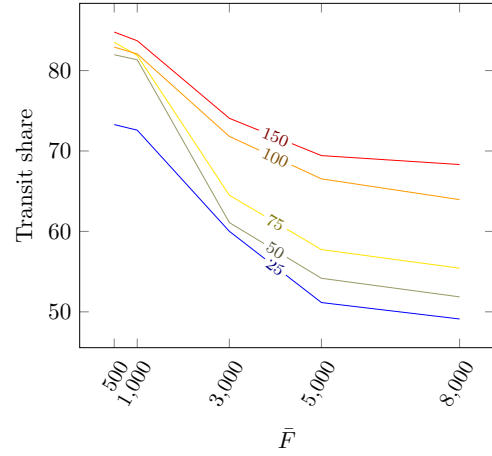


(d) Total expected travel cost (pass-hrs)

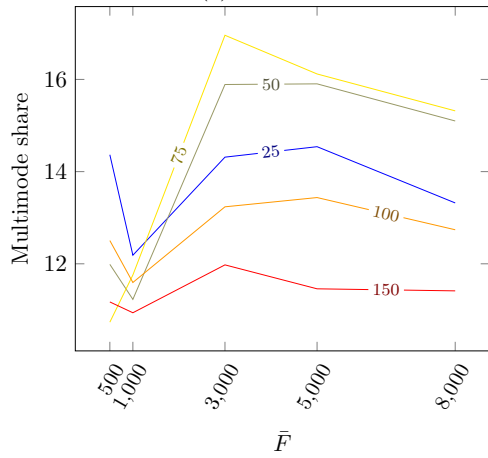
Figure 5: Sensitivity of parameters  $\bar{F}$  and  $\bar{B}$  on different costs (contour represents varying bus fleet sizes)



(a) MoD share



(b) Transit share



(c) Multimode share

Figure 6: Sensitivity of parameters  $\bar{F}$  and  $\bar{B}$  on mode share (contour represents varying bus fleet sizes)

557 *6.5. Comparison of optimized base transit system with proposed integrated system*

558 In this section, we present a comparison of the operation of the "optimized base transit system"  
 559 corresponding to the existing transit system with optimized frequencies versus the design of the  
 560 integrated system evaluated in §6.2. For the optimized base case, we solve the optimization program  
 561 (18) for the instance described in §6.1. The results of optimized frequencies of various routes are  
 562 given in Table 6. The network provides an average wait time of 18 minutes to the passengers.

$$\begin{aligned} \underset{v, W, y}{\text{minimize}} \quad & \sum_{k \in D} \left( \sum_{a \in A} c_a v_{ak} + \sum_{i \in N_T^w} W_{ik} \right) \end{aligned} \quad (18a)$$

$$\text{subject to} \quad \sum_{l \in L} \sum_{f \in \Theta} \mathcal{B}(l, f) \times y_{lf} \leq \bar{B} \quad (18b)$$

$$\sum_{a \in FS(i)} v_{ak} = \sum_{a \in BS(i)} v_{ak} + g_{ik}, \forall i \in N, \forall k \in D \quad (18c)$$

$$v_{ak} \leq \left( \sum_{f \in \Theta} f y_{l(a)f} \right) W_{ik}, \forall a \in FS(i) : a \in A_T, \forall i \in N^w, \forall k \in D \quad (18d)$$

$$v_{ak} \geq 0, \forall a \in A, \forall k \in D \quad (18e)$$

$$W_{ik} \text{ free}, \forall i \in N_T^w, \forall k \in D \quad (18f)$$

$$y_{lf} \in \mathfrak{B}, \forall f \in \Theta, \forall l \in L \quad (18g)$$

Table 6: Routes with their optimal frequency (optimized base case)

Route	Optimal frequency (buses/hr)	Average wait time (min)
1	4	15
2	2	30
3	6	10
4	12	5
5	3	20
6	2	30
7	3	20
8	3	20
9	3	20
10	2	30
11	12	5
12	6	10

563 The results comparing the performance of the optimized base transit system and integrated  
564 system are provided in Table 7. The base transit system has 12 two-way bus services operated by a  
565 bus fleet of 69 buses, whereas the new integrated system has 6 two-way bus services operated by 69  
566 buses. Along with 69 buses, the new integrated system deploys 3,000 vehicles to serve the demand.  
567 The deployment of these extra vehicles can be costly to the transportation agencies. However, they  
568 provide several benefits. First, the optimized base transit system is not able to serve 13 % of the  
569 demand due to the non-availability of transit service in 2 zones in the network. On the other hand,  
570 the first mile and last mile of these zones are covered by vehicles in the integrated system. Second,  
571 the average in-vehicle travel time of passengers using the integrated system is only 14.43 minutes  
572 in comparison to the 21.16 minutes for passengers using the base transit system. However, the

573 average wait time of the integrated system users is increased slightly in comparison to the base  
 574 transit system. This is due to the increased number of transfers to access MoD and transit service.

Table 7: Comparison of optimized base transit system and integrated system

	<b>Optimized base transit system</b>	<b>Integrated system</b>
Number of active routes	12	6
Number of buses used	69	69
Number of vehicles used	0	3,000
Satisfied demand (%)	87	100
Average in-vehicle time (min/passenger)	21.16	14.43
Average wait time (min/passenger)	2.88	4.37

### 575 6.6. Managerial insights for implementing such service

576 For implementing the proposed model in practice, we need to follow the following procedure.  
 577 First, we divide the region into zones. Second, we collect the peak hour demand data in the region.  
 578 Third, solve the proposed design model for varying fleet sizes. This step will be similar to the  
 579 sensitivity analysis given in Section 6.4. This analysis will help us decide the optimal fleet size of  
 580 buses and vehicles for our service. It will also provide us with the allocation of vehicles and buses  
 581 for different zones and bus routes respectively. This allocation is designed for peak hours. We  
 582 can reduce the vehicle operation in non-peak hours. For the bus service, scheduling needs to be  
 583 performed to publish a schedule for the service.

## 584 7. Conclusions and Future Research

585 Advances in mobility services have paved the way for the development of a new type of MoD  
 586 service, which can help in serving the first mile and last mile of transit trips. Such a system requires  
 587 rethinking the design of a transit system that allows for intermodal trips with MoD as the first  
 588 or last leg of trips. We developed a mixed-integer non-linear program (MINLP) to design such  
 589 system. The MINLP was relaxed to a mixed-integer linear program with the help of McCormick  
 590 relaxations. To solve the resulting MILP model efficiently, we proposed the Benders decomposition  
 591 method with several enhancements. These enhancements include the use of disaggregated cuts,  
 592 clique/cover cuts, and multiple cuts via multiple solutions. The numerical results show that disag-  
 593 gregated cuts with clique/cover cuts and multiple cuts via multiple solutions are efficient techniques  
 594 to solve the current problem. Furthermore, the experiment results on the Sioux Falls network show  
 595 that the congestion in the city center is improved with such design as most of the passengers were  
 596 found to take the transit in that region. The sensitivity analysis on bus fleet size and vehicle fleet  
 597 size shows that the passenger hours spent in the system as in-vehicle time and wait time reduces  
 598 with an increase in the number of available buses and vehicles. The share of multimodal service  
 599 was observed to be highest for the vehicle fleet size and bus fleet size of 3,000 and 75 respectively.  
 600 We also compared the proposed integrated system with the optimized base transit system. We

601 found that the integrated system can be costly due to the deployment of vehicles, but it reduces  
602 the passenger in-vehicle time and serves more demand than the optimized base case.

603

604 This research can be expanded in multiple directions. First, ridepooling was not allowed in  
605 the current study. Further research is needed to explore the ideas of including the matching of  
606 passengers for ridepooling, which will further reduce the size of the vehicle fleet required to provide  
607 the service. Second, better calibration of parameter  $\mathcal{A}$  used in the wait time computation of MoD  
608 service is needed. The data from ridehailing services can be used for this purpose.

## 609 **Acknowledgments**

610 This research is conducted at the University of Minnesota Transit Lab, currently supported by  
611 the following, but not limited to, projects:

612 - National Science Foundation, award CMMI-1831140

613 - Freight Mobility Research Institute (FMRI), Tier 1 Transportation Center, U.S. Department  
614 of Transportation: award RR-K78/FAU SP#16-532 AM2 and AM3

615 - Minnesota Department of Transportation, Contract No. 1003325 Work Order No. 44 and  
616 111

617 - University of Minnesota Office of Vice President for Research, COVID-19 Rapid Response  
618 Grants



619 **References**

- 620 Aftabuzzaman, M., Currie, G. and Sarvi, M. 2015, 'Evaluating the Congestion Relief Impacts of  
621 Public Transport in Monetary Terms', *Journal of Public Transportation* **13**(1), 1–24.
- 622 Baaj, M. H. and Mahmassani, H. S. 1991, 'An AI-based approach for transit route system planning  
623 and design', *Journal of advanced transportation* **25**(2), 187–209.
- 624 Basu, R., Araldo, A., Akkinepally, A. P., Nahmias Biran, B. H., Basak, K., Seshadri, R., Deshmukh,  
625 N., Kumar, N., Azevedo, C. L. and Ben-Akiva, M. 2018, 'Automated Mobility-on-Demand vs.  
626 Mass Transit: A Multi-Modal Activity-Driven Agent-Based Simulation Approach', *Transporta-  
627 tion Research Record* **2672**(8), 608–618.  
628 **URL:** <https://doi.org/10.1177/0361198118758630>
- 629 Beheshti Asl, N. and MirHassani, S. A. 2019, 'Accelerating benders decomposition: multiple cuts  
630 via multiple solutions', *Journal of Combinatorial Optimization* **37**(3), 806–826.  
631 **URL:** <https://doi.org/10.1007/s10878-018-0320-8>
- 632 Benders, J. F. 1962, 'Partitioning procedures for solving mixed-variables programming problems',  
633 *Numerische Mathematik* **4**(1), 238–252.
- 634 Bian, Z. and Liu, X. 2019, 'Mechanism design for first-mile ridesharing based on personalized  
635 requirements part I: Theoretical analysis in generalized scenarios', *Transportation Research Part  
636 B: Methodological* **120**, 147–171.  
637 **URL:** <https://doi.org/10.1016/j.trb.2018.12.009>
- 638 Campbell, J. F., Ernst, A. T. and Krishnamoorthy, M. 2005a, 'Hub arc location problems: Part I  
639 - Introduction and results', *Management Science* **51**(10), 1540–1555.
- 640 Campbell, J. F., Ernst, A. T. and Krishnamoorthy, M. 2005b, 'Hub Arc location problems: Part II  
641 - Formulations and optimal algorithms', *Management Science* **51**(10), 1556–1571.
- 642 Cayford, R. and Yim, Y. B. Y. 2004, 'Personalized Demand-Responsive Transit Service'.
- 643 Ceder, A. and Wilson, N. H. M. 1986, 'Bus network design', *Transportation Research Part B:  
644 Methodological* **20**(4), 331–344.  
645 **URL:** <http://www.sciencedirect.com/science/article/pii/0191261586900470>
- 646 Cepeda, M., Cominetti, R. and Florian, M. 2006, 'A frequency-based assignment model for con-  
647 gested transit networks with strict capacity constraints: characterization and computation of  
648 equilibria', *Transportation research part B: Methodological* **40**(6), 437–459.
- 649 Chen, S., Wang, H. and Meng, Q. 2020, 'Solving the first-mile ridesharing problem using au-  
650 tonomous vehicles', *Computer-Aided Civil and Infrastructure Engineering* **35**(1), 45–60.

- 651 Chen, T. D. and Kockelman, K. M. 2016, ‘Management of a shared autonomous electric vehicle  
652 fleet: Implications of pricing schemes’, *Transportation Research Record* **2572**(2572), 37–46.
- 653 Cominetti, R. and Correa, J. 2001, ‘Common-lines and passenger assignment in congested transit  
654 networks’, *Transportation Science* **35**(3), 250–267.
- 655 Conforti, M., Cornuejols, G. and Zambelli, G. 2014, *Integer Programming*, Graduate Texts in  
656 Mathematics, Springer International Publishing.  
657 **URL:** <https://books.google.com/books?id=KUHUoAEACAAJ>
- 658 De Cea, J. and Fernández, E. 1993, ‘Transit assignment for congested public transport systems: an  
659 equilibrium model’, *Transportation science* **27**(2), 133–147.
- 660 Desaulniers, G. and Hickman, M. D. 2007, ‘Chapter 2 Public Transit’, *Handbooks in Operations  
661 Research and Management Science* **14**(C), 69–127.
- 662 Douglas, G. W. 1972, ‘Price Regulation and Optimal Service Standards: The Taxicab Industry’,  
663 *Journal of Transport Economics and Policy* **6**(2), 116–127.  
664 **URL:** <http://www.jstor.org/stable/20052271>
- 665 Fagnant, D. J., Kockelman, K. M. and Bansal, P. 2016, ‘Operations of Shared Autonomous Vehicle  
666 Fleet for Austin, Texas, Market’, *Transportation Research Record* **2563**(1), 98–106.  
667 **URL:** <https://doi.org/10.3141/2536-12>
- 668 Gentile, G., Nguyen, S. and Pallottino, S. 2005, ‘Route choice on transit networks with online  
669 information at stops’, *Transportation science* **39**(3), 289–297.
- 670 Geoffrion, A. M. 1972, ‘Generalized Benders decomposition’, *Journal of Optimization Theory and  
671 Applications* **10**(4), 237–260.  
672 **URL:** <https://doi.org/10.1007/BF00934810>
- 673 Guihaire, V. and Hao, J. K. 2008, ‘Transit network design and scheduling: A global review’,  
674 *Transportation Research Part A: Policy and Practice* **42**(10), 1251–1273.  
675 **URL:** <http://dx.doi.org/10.1016/j.tra.2008.03.011>
- 676 Gurumurthy, K. M., Kockelman, K. M. and Zuniga-Garcia, N. 2020, ‘First-Mile-Last-Mile  
677 Collector-Distributor System using Shared Autonomous Mobility’, *Transportation Research  
678 Record* **0**(0), 0361198120936267.  
679 **URL:** <https://doi.org/10.1177/0361198120936267>
- 680 Khani, A., Lee, S., Hickman, M., Noh, H. and Nassir, N. 2012, ‘Intermodal Path Algorithm for  
681 Time-Dependent Auto Network and Scheduled Transit Service’, *Transportation Research Record:  
682 Journal of the Transportation Research Board* **2284**(2284), 40–46.  
683 **URL:** <http://trrjournalonline.trb.org/doi/10.3141/2284-05>

- 684 Koffman, D. 2004, *Operational Experiences with Flexible Transit Services*, National Academies  
685 Press.
- 686 Kumar, P. and Khani, A. 2021, ‘An algorithm for integrating peer-to-peer ridesharing and schedule-  
687 based transit system for first mile/last mile access’, *Transportation Research Part C: Emerging  
688 Technologies* **122**, 102891.  
689 **URL:** <https://www.sciencedirect.com/science/article/pii/S0968090X20307919>
- 690 Kurauchi, F., Bell, M. G. and Schmöcker, J. D. 2003, ‘Capacity Constrained Transit Assignment  
691 with Common Lines’, *Journal of Mathematical Modelling and Algorithms* **2**(4), 309–327.
- 692 Laris, M. 2019, ‘Uber and Lyft concede they play role in traffic congestion in the District and other  
693 urban areas’.  
694 **URL:** [https://www.washingtonpost.com/transportation/2019/08/06/uber-lyft-concede-they-play-  
695 role-traffic-congestion-district-other-urban-areas/](https://www.washingtonpost.com/transportation/2019/08/06/uber-lyft-concede-they-play-role-traffic-congestion-district-other-urban-areas/)
- 696 Larson, R. C. and Odoni, A. R. 1981, *Urban operations research*, number Monograph, 2nd editio  
697 edn, Dynamic Ideas.
- 698 Lee, A. and Savelsbergh, M. 2017, ‘An extended demand responsive connector’, *EURO Journal on  
699 Transportation and Logistics* **6**(1), 25–50.  
700 **URL:** <http://dx.doi.org/10.1007/s13676-014-0060-6>
- 701 Leurent, F., Chandakas, E. and Poulhès, A. 2014, ‘A traffic assignment model for passenger tran-  
702 sit on a capacitated network: Bi-layer framework, line sub-models and large-scale application’,  
703 *Transportation Research Part C: Emerging Technologies* **47**(P1), 3–27.  
704 **URL:** <http://dx.doi.org/10.1016/j.trc.2014.07.004>
- 705 Levin, M. W. and Boyles, S. D. 2015, ‘Effects of autonomous vehicle ownership on trip, mode, and  
706 route choice’, *Transportation Research Record* **2493**, 29–38.
- 707 Levin, M. W., Kockelman, K. M., Boyles, S. D. and Li, T. 2017, ‘A general framework for modeling  
708 shared autonomous vehicles with dynamic network-loading and dynamic ride-sharing applica-  
709 tion’, *Computers, Environment and Urban Systems* **64**, 373–383.  
710 **URL:** <http://dx.doi.org/10.1016/j.compenvurbsys.2017.04.006>
- 711 Li, X. and Quadrifoglio, L. 2009, ‘Optimal Zone Design for Feeder Transit Services’, *Transportation  
712 Research Record: Journal of the Transportation Research Board* **2111**(1), 100–108.
- 713 Liu, Y., Bansal, P., Daziano, R. and Samaranayake, S. 2019, ‘A framework to integrate mode  
714 choice in the design of mobility-on-demand systems’, *Transportation Research Part C: Emerging  
715 Technologies* **105**, 648–665.  
716 **URL:** <https://www.sciencedirect.com/science/article/pii/S0968090X18313718>

- 717 Ma, T. Y., Rasulkhani, S., Chow, J. Y. and Klein, S. 2019, ‘A dynamic ridesharing dispatch and idle  
718 vehicle repositioning strategy with integrated transit transfers’, *Transportation Research Part E:  
719 Logistics and Transportation Review* **128**(July), 417–442.  
720 **URL:** <https://doi.org/10.1016/j.tre.2019.07.002>
- 721 Magnanti, T. L. and Wong, R. T. 1981, ‘Accelerating Benders Decomposition: Algorithmic En-  
722 hancement and Model Selection Criteria’, *Operations Research* **29**(3), 464–484.  
723 **URL:** <https://doi.org/10.1287/opre.29.3.464>
- 724 Maheo, A., Kilby, P. and Van Hentenryck, P. 2017, ‘Benders decomposition for the design of a hub  
725 and shuttle public transit system’, *Transportation Science* **53**(1), 77–88.
- 726 Mahéo, A., Kilby, P. and Van Hentenryck, P. 2019, ‘Benders decomposition for the design of a hub  
727 and shuttle public transit system’, *Transportation Science* **53**(1), 77–88.
- 728 Manser, P. 2017, Public Transport Network Design in a World of Autonomous Vehicles, PhD thesis,  
729 Master thesis.
- 730 Masoud, N., Nam, D., Yu, J. and Jayakrishnan, R. 2017, ‘Promoting Peer-to-Peer Ridesharing Ser-  
731 vices as Transit System Feeders’, *Transportation Research Record: Journal of the Transportation  
732 Research Board* **2650**, 74–83.  
733 **URL:** <http://trrjournalonline.trb.org/doi/10.3141/2650-09>
- 734 Mendes, L. M., Bennàssar, M. R. and Chow, J. Y. 2017, ‘Comparison of light rail streetcar against  
735 shared autonomous vehicle fleet for Brooklyn–Queens connector in New York City’, *Transporta-  
736 tion Research Record* **2650**(1), 142–151.  
737 **URL:** <https://doi.org/10.3141/2650-17>
- 738 Mo, B., Cao, Z., Zhang, H., Shen, Y. and Zhao, J. 2020, ‘Dynamic Interaction between Shared  
739 Autonomous Vehicles and Public Transit: A Competitive Perspective’, **100084**.  
740 **URL:** <http://arxiv.org/abs/2001.03197>
- 741 Motavalli, J. 2020, ‘Who Will Own the Cars That Drive Themselves?’.  
742 **URL:** [https://www.nytimes.com/2020/05/29/business/ownership-autonomous-cars-  
743 coronavirus.html](https://www.nytimes.com/2020/05/29/business/ownership-autonomous-cars-coronavirus.html)
- 744 Nassir, N., Khani, A., Hickman, M. and Noh, H. 2012, ‘Algorithm for Intermodal Optimal Multi-  
745 destination Tour with Dynamic Travel Times’, *Transportation Research Record: Journal of the  
746 Transportation Research Board* **2283**, 57–66.  
747 **URL:** <http://trrjournalonline.trb.org/doi/10.3141/2283-06>
- 748 OECD 2015, ‘Urban Mobility System Upgrade: How shared self-driving cars could change city  
749 traffic’, *Corporate Partnership Board Report* pp. 1–36.  
750 **URL:** [http://www.internationaltransportforum.org/Pub/pdf/15CPB\\_Self-drivingcars.pdf](http://www.internationaltransportforum.org/Pub/pdf/15CPB_Self-drivingcars.pdf)

- 751 Pinto, H. K., Hyland, M. F., Mahmassani, H. S. and Verbas, I. Ö. 2020, ‘Joint design of multi-  
752 modal transit networks and shared autonomous mobility fleets’, *Transportation Research Part*  
753 *C: Emerging Technologies* **113**(June), 2–20.
- 754 Quadrifoglio, L., Dessouky, M. M. and Ordóñez, F. 2008, ‘A simulation study of demand responsive  
755 transit system design’, *Transportation Research Part A: Policy and Practice* **42**(4), 718–737.
- 756 Saharidis, G. K. and Ierapetritou, M. G. 2010, ‘Improving benders decomposition using maxi-  
757 mum feasible subsystem (MFS) cut generation strategy’, *Computers and Chemical Engineering*  
758 **34**(8), 1237–1245.
- 759 Salazar, M., Rossi, F., Schiffer, M., Onder, C. H. and Pavone, M. 2018, On the Interaction between  
760 Autonomous Mobility-on-Demand and Public Transportation Systems, in ‘2018 21st Interna-  
761 tional Conference on Intelligent Transportation Systems (ITSC)’, pp. 2262–2269.
- 762 Shen, C.-W. and Quadrifoglio, L. 2012, ‘Evaluation of Zoning Design with Transfers for Para-  
763 transit Services’, *Transportation Research Record: Journal of the Transportation Research Board*  
764 **2277**(1), 82–89.
- 765 Shen, Y., Zhang, H. and Zhao, J. 2018, ‘Integrating shared autonomous vehicle in public trans-  
766 portation system: A supply-side simulation of the first-mile service in Singapore’, *Transportation*  
767 *Research Part A: Policy and Practice* **113**(March), 125–136.
- 768 Spiess, H. and Florian, M. 1989, ‘Optimal strategies: A new assignment model for transit networks’,  
769 *Transportation Research Part B* **23**(2), 83–102.
- 770 Steiner, K. and Irnich, S. 2020, ‘Strategic Planning for Integrated Mobility-on-Demand and Urban  
771 Public Bus Networks’, *Transportation Science* **54**(6), 1616–1639.  
772 **URL:** <https://doi.org/10.1287/trsc.2020.0987>
- 773 Stiglic, M., Agatz, N., Savelsbergh, M. and Gradisar, M. 2018, ‘Enhancing urban mobility: Inte-  
774 grating ride-sharing and public transit’, *Computers and Operations Research* **90**, 12–21.  
775 **URL:** <http://dx.doi.org/10.1016/j.cor.2017.08.016>
- 776 Szeto, W. Y. and Jiang, Y. 2014, ‘Transit route and frequency design: Bi-level modeling and  
777 hybrid artificial bee colony algorithm approach’, *Transportation Research Part B: Methodological*  
778 **67**, 235–263.  
779 **URL:** <http://dx.doi.org/10.1016/j.trb.2014.05.008>
- 780 Tang, L., Jiang, W. and Saharidis, G. K. 2013, ‘An improved Benders decomposition algorithm for  
781 the logistics facility location problem with capacity expansions’, *Annals of Operations Research*  
782 **210**(1), 165–190.
- 783 Vakayil, A., Gruel, W. and Samaranyake, S. 2017, Integrating shared-vehicle mobility-on-demand  
784 systems with public transit, Technical report, Transportation Research Board, Washington, D.C.

- 785 Wang, H. 2017, ‘Routing and Scheduling for a Last-Mile Transportation System’, *Transportation*  
786 *Science* **53**(December 2018), trsc.2017.0753.  
787 **URL:** <http://pubsonline.informs.org/doi/10.1287/trsc.2017.0753>
- 788 Webb, A. and Khani, A. 2020, ‘Park-and-Ride Choice Behavior in a Multimodal Network with  
789 Overlapping Routes’, *Transportation Research Record* **2674**(3), 150–160.  
790 **URL:** <https://doi.org/10.1177/0361198120908866>
- 791 Wen, J., Chen, Y. X., Nassir, N. and Zhao, J. 2018, ‘Transit-oriented autonomous vehicle oper-  
792 ation with integrated demand-supply interaction’, *Transportation Research Part C: Emerging*  
793 *Technologies* **97**(January), 216–234.  
794 **URL:** <https://doi.org/10.1016/j.trc.2018.10.018>
- 795 Wilson, W. H. 1972, ‘Statewide Intermodal Transportation Planning in the Less Urbanized State’,  
796 *Highway Research Record* (401).
- 797 Yin, Y. 2019, ‘Macroscopic modeling of ridesourcing systems - Regulations and Fundamental Dia-  
798 gram’.  
799 **URL:** <https://www.youtube.com/watch?v=oiBhwJl5xXc&t=717s>
- 800 Zha, L., Yin, Y. and Yang, H. 2016, ‘Economic analysis of ride-sourcing markets’, *Transportation*  
801 *Research Part C: Emerging Technologies* **71**, 249–266.  
802 **URL:** <http://dx.doi.org/10.1016/j.trc.2016.07.010>

## 803 **Appendix A Proofs of various propositions**

### 804 **Proof of Proposition 1**

805 (Although the proof can be found in Spiess and Florian 1989 or Gentile et al. 2005, we repeat it  
806 here because some of the details presented here will be used in proving the next proposition.) The  
807 probability of choosing line  $i \in FS(n)$  is equal to the probability of waiting time for line  $i \in FS(n)$   
808 to be less than or equal to waiting time of other lines  $j \neq i$ , i.e.,

$$P_i = Prob(w_i \leq \min_{j \neq i} w_j) = \int_0^\infty g_i(w) \prod_{j \neq i} Prob(w_j \geq w) dw = \int_0^\infty \gamma_i(w) dw \quad (19)$$

809 where,  $\gamma_i(w) = g_i(w) \prod_{j \neq i} Prob(w_j \geq w) = f_i e^{-f_i w} \prod_{j \neq i} e^{-f_j w} = f_i e^{-(\sum_j f_j)w}$ . The value of  $\gamma_i(w)$   
810 can be interpreted as the probability density function of the waiting time at the stop  $n$  conditional  
811 to boarding line  $i$ . Using (19), the probability of choosing line  $i \in FS(n)$  can be evaluated as:

$$P_i = \int_0^\infty f_i e^{-(\sum_j f_j)w} dw = \frac{f_i}{\mathfrak{F}} \quad (20)$$

812 The expected wait time conditional to boarding line  $i$  is:

$$EW_i = \int_0^\infty w\gamma_i(w)dw = \int_0^\infty wf_i e^{-(\sum_j f_j)w} dw = \frac{f_i}{\mathfrak{F}^2} \quad (21)$$

813 Summing over all the lines  $FS(n)$  gives us the expected wait time at the stop, i.e.,

$$EW_n = \sum_{i \in FS(n)} \int_0^\infty w\gamma_i(w)dw = \int_0^\infty w \sum_i \gamma_i(w)dw \quad (22)$$

814 where,  $\sum_i \gamma_i(w)$  is the probability density function of the waiting time at stop  $n$ .

$$\sum_{i \in FS(n)} \gamma_i(w) = \sum_{i \in FS(n)} f_i e^{-(\sum_j f_j)w} = \mathfrak{F} e^{-\mathfrak{F}w}, w \geq 0 \quad (23)$$

815 Therefore, the expected wait time at stop  $n$  is given by  $EW_n = \frac{1}{\mathfrak{F}}$

816

### 817 **Proof of Proposition 2**

818 The probability of taking transit is given by:

$$P_{transit} = \int_0^\infty \left( \sum_i \gamma_i(w) \right) Prob(w \leq w_{MoD}) dw \quad (24)$$

$$P_{transit} = \int_0^\infty \mathfrak{F} e^{-\mathfrak{F}w} \times e^{-(f_{MoD})w} dw = \frac{\mathfrak{F}}{\mathbb{F}} \quad (25)$$

$$(26)$$

819 Similarly, the probability of taking MoD is given by  $P_{MoD} = \frac{\mathfrak{F}}{\mathbb{F}}$ . The expected wait time of the  
820 passenger departing from an access node  $n$  is given by:

$$EW_n = \int_0^\infty w \left( \mathfrak{F} e^{-(f_{MoD} + \mathfrak{F})w} + f_{MoD} e^{-(f_{MoD} + \mathfrak{F})w} \right) dw = \frac{1}{\mathbb{F}} \quad (27)$$

821

822

823 **Proof of Proposition 3** To prove this, we need to show that (a)  $proj_{v,W} \mathcal{X}^{SP} \subseteq \mathcal{X}^{MA}$  and  
824 (b)  $\mathcal{X}^{MA} \subseteq proj_{v,W} \mathcal{X}^{SP}$ . Let us first start by proving (b). Let  $(v, W) \in \mathcal{X}^{MA}$ . For all  
825  $a \in FS(i) : a \in A_T, \forall i \in N^w, \forall k \in D$ , we have  $v_{ak} \leq f_a W_{ik}$ . Let  $y_{l(a)f} = 1$  if the fre-  
826 quency of the line associated to arc  $a$  is  $f \in \Theta$  and 0, otherwise. Let  $t_{faik} = \hat{y}_{l(a)f} W_{ik}$ , then  
827  $f_a W_{ik} = \sum_{f \in \Theta} f \hat{y}_{l(a)f} W_{ik} = \sum_{f \in \Theta} f t_{faik}$ , which is same as (14c). Also,  $t_{faik} = \hat{y}_{l(a)f} W_{ik}$  can  
828 be expressed as (14d)- (14f) and (14l). Using a similar argument, we can show that for all  
829  $a \in FS(i) : a \in A_R, \forall i \in N^w, \forall k \in D$ , the inequality  $v_{ak} \leq f_a W_{ik}$  can be expressed as (14g)-  
830 (14j) and (14m). This shows that  $\mathcal{X}^{MA} \subseteq proj_{v,W} \mathcal{X}^{SP}$ . To prove part (a), let  $(v, W, \omega, t) \in \mathcal{X}^{SP}$ ,  
831 then using Fourier-Motzkin elimination, we have  $(v, W) \in \mathcal{X}^{MA}$  (Conforti et al. 2014, Chapter 3).

832

833 **Proof of Proposition 4** The set  $\mathcal{X}^{SP}$  can be empty in two cases i.e., when there is no flow  
834 balance ( $\sum_{k \in D} \sum_{i \in N} g_{ik} \neq 0$ ) or there does not exist a directed path from any node  $i \in N$  to any

835 destination  $k$ . However, it is not possible to have any of these cases because from the definition of  
836  $g_{ik}$ , we have  $\sum_{k \in D} \sum_{i \in N} g_{ik} = 0$  and since there is always at least 0.01 vehicle assigned to all the  
837 zones and the road network is connected, there always exists a path from any node  $i \in N$  to any  
838 destination  $k \in D$ . Therefore,  $\mathcal{X}^{SP} \neq \phi$ .

839 **Proof of Proposition 5** Due to limited fleet available, one can allocate  $n \in \Omega$  vehicles in at most  
840  $\lfloor \frac{\bar{F}}{n} \rfloor$  zones.

841 **Proof of Proposition 6** The proposition follows from the definition of minimal cover that we  
842 cannot provide the number of buses required in the minimal cover.